



ADVANCED MASTERS IN STRUCTURAL ANALYSIS  
OF MONUMENTS AND HISTORICAL CONSTRUCTIONS



# Master's Thesis

Maïa Laffineur

## **Optimization of a computational model for the restoration of the intrados of the Charles Bridge (Prague)**

This Masters Course has been funded with support from the European Commission. This publication reflects the views only of the author, and the Commission cannot be held responsible for any use which may be made of the information contained therein.





**CZECH TECHNICAL UNIVERSITY IN PRAGUE**

Faculty of Civil Engineering

Thákurova 7, 166 29 Prague 6, Czech Republic

## MASTER'S THESIS PROPOSAL

study programme: Civil Engineering  
study branch: Advanced Masters in Structural Analysis of Monuments and Historical Constructions  
academic year: 2016/2017


Student's name and surname: LAFFINEUR Mařa  
Department: Department of Mechanics  
Thesis supervisor: HAVLASEK Petr  
Thesis title: Optimization of a computational model for the restoration of the intrados of the Charles Bridge (Prague)  
Thesis title in English: see above

Framework content: The thesis focuses on the development of a finite element model of the intrados of the 14th arch of the Charles Bridge in order to optimize the replacement of damaged stones without causing a too important global deformation or local increase of stress.

Assignment date: 7/04/2017 Submission date: 06/07/2017

If the student fails to submit the Master's thesis on time, they are obliged to justify this fact in advance in writing, if this request (submitted through the Student Registrar) is granted by the Dean, the Dean will assign the student a substitute date for holding the final graduation examination (2 attempts for FGE remain). If this fact is not appropriately excused or if the request is not granted by the Dean, the Dean will assign the student a date for retaking the final graduation examination, FGE can be retaken only once. (Study and Examination Code, Art 22, Par 3, 4.)

*The student takes notice of the obligation of working out the Master's thesis on their own, without any outside help, except for consultation. The list of references, other sources and names of consultants must be included in the Master's thesis.*

  
Master's thesis supervisor

  
Head of department

Date of Master's thesis proposal take over: July 2017

Student 

This form must be completed in 3 copies – 1x department, 1x student, 1x Student Registrar (sent by department)

No later than by the end of the 2<sup>nd</sup> week of instruction in the semester, the department shall send one



## DECLARATION

Name: Maïa LAFFINEUR

Email: maia.laffineur@ens-paris-saclay.fr

Title of the Msc Dissertation: Optimization of a computational model for the restoration of the intrados of the Charles Bridge (Prague)

Supervisor(s): Petr Havlásek

Year: 2017

I hereby declare that all information in this document has been obtained and presented in accordance with academic rules and ethical conduct. I also declare that, as required by these rules and conduct, I have fully cited and referenced all material and results that are not original to this work.

I hereby declare that the MSc Consortium responsible for the Advanced Masters in Structural Analysis of Monuments and Historical Constructions is allowed to store and make available electronically the present MSc Dissertation.

University: Czech Technical University in Prague

Date: 04/07/2017

Signature: Maïa Laffineur



## Acknowledgments

My sincere gratitude goes to Petr Havlásek for his kind supervision, for his availability and all the valuable technical and personal advices he shared during the preparation and the writing of this thesis.

I would also like to thank Professor Bořek Patzák who was of great help to fix computational problems. Daniel Ryppl kindly allowed me to use the software T3D he developed.

I am also grateful to Dušan Drahoš who provided the blueprints and reports of the site investigation of the Charles Bridge.

This thesis is the accomplishment of the Advanced Masters in Structural Analysis of Monuments and Historical Constructions that was a very rich formation to gather specific knowledge. I would like to thank the University of Padova and the Technical University of Czech Republic in Prague for welcoming me, as well as the University of Minho who organized the year. I realize the efforts made by the administration and the lecturers to transmit their passion about cultural heritage, and especially Pr. Maria Rosa Valluzzi, Pr. Petr Kabele and Pr. Paulo B. Lourenço.

This experience has been possible thanks to the SAHC Consortium major financial support, for which I'm truly grateful.

My thoughts also go to the people who supported me, my classmates, my relative and parents, but also the people I met both in Italy and Czech Republic. Blessed be the Lord who guides me with unconditional Love through life.





## Abstract

### Optimization of a computational model for the restoration of the intrados of the Charles Bridge (Prague)

The Charles Bridge is one of the symbols of Prague. This monument constitutes one of the jewels of Gothic structures and is classified by the UNESCO. Ordered by Charles IV in the 14th century, it laid until the end of the 19th century on an important trade road crossing the Holy Roman Empire. It suffered from severe damages through centuries. Amongst them can be mentioned the collapse of pillars due to floods, as well as chemical deterioration due to water infiltration. Nowadays, the parts that require the most urgent attention are the intrados of the arches.

As a part of preliminary study to prepare the restoration of the intrados, the present work aims at developing and optimizing a computational model to understand the behavior of the arches when replacing the damaged stone units. The specificity of such modeling is closely linked to the construction stages and changes in the statical scheme. Finite elements constituting the damaged stone blocks vanish, then other elements of the new unit appear – they have the same topology, but different properties and loading. Finally, the transfer of stress from the structure to the new stone, what can be called the reactivation, is delicate to model properly. For this purpose, two models are developed. One, homogeneous, can describe the complete procedure. The other one, reflecting the mesostructure of the masonry, is more suitable to capture the reactivation phenomenon.

A representative area of the most damaged arch is investigated by means of a linear finite element analysis and the most influencing factors are determined. The target criteria are the minimum deformation of the arch and the minimum stress increase in the surrounding stones in the repaired area.

**Keywords:** stone masonry, historical heritage, Finite Element Method, restoration techniques, construction stages

## Abstrakt

### Optimalizace výpočetního modelu pro obnovu klenby Karlova mostu v Praze

Karlův most je jeden ze symbolů Prahy. Tento monument představuje jeden z klenotů gotické architektury a je zařazen na seznam UNESCO. Ač jeho stavba byla nařízena Karlem IV. ve 14. století, nacházel se až do konce 19. století na významné obchodní cestě Svaté říše římské. Během staletí byl most mnohokrát vážně poškozen. Mimo jiné může být zmíněno zřícení pilířů při povodních a chemická degradace způsobená prosakováním vody. V současné době vyžadují urgentní péči klenby mostních oblouků.

Součástí předběžné studie pro přípravu obnovy klenby mostu je tato práce, která je zaměřena na vývoj a optimalizaci výpočetního modelu sloužícího pro porozumění chování oblouku při výměně poškozených kamenných jednotek. Modelování tohoto procesu je specifické úzkým spojením s postupem výstavby a změnami statického schématu. Konečné prvky tvořící poškozené kamenné bloky mizí, ale jiné, mající stejnou topologii, ale jiné vlastnosti a zatížení, se objevují. Modelování přenosu napětí z konstrukce do nového kamene (aktivace), je obtížné správně vystihnout. Za tímto účelem byly vytvořeny dva modely. První homogenní model může vhodně popsat celý proces výměny. Druhý model odráží mesostrukturu zdiva a je vhodnější pro popis aktivace.

Reprezentativní oblast nejvíce poškozeného mostního oblouku je prozkoumána pomocí lineární metody konečných prvků a jsou určeny nejvíce ovlivňující faktory. Cílovými kritérii jsou minimální deformace oblouku a zvýšení napětí v blocích v opravované oblasti.

**Klíčová slova:** kamenné zdivo, historické dědictví, metoda konečných prvků, techniky obnovy, fáze výstavby

## Résumé

### Optimisation d'un modèle numérique pour la restauration des intrados du Pont Charles (Prague)

Le Pont Charles est un des symboles de Prague. Ce monument constitue un des joyaux de l'architecture gothique et est classé au patrimoine mondial de l'UNESCO. Construit au XIV<sup>e</sup> s. à la demande de Charles IV, il se trouve jusqu'à la fin du XIX<sup>e</sup> s. sur une importante voie marchande qui traverse le Saint Empire Romain Germanique. Il connut au cours des siècles de nombreux dommages, parmi lesquels l'effondrement de certaines piles suite à des inondations ainsi que de l'érosion chimique suite aux infiltrations d'eau. De nos jours, les intrados des arcs sont les éléments les plus abîmés et nécessitent donc une intervention urgente.

Dans le cadre d'une étude préliminaire pour préparer la restauration des intrados, le travail actuel a pour but le développement et l'optimisation d'un modèle numérique permettant de comprendre le comportement des arcs pendant le changement des pierres. La spécificité d'une telle modélisation est liée à la présence de plusieurs phases de construction et aux changements statiques de chacune de ces phases. Les éléments finis qui constituent les pierres endommagées disparaissent, puis d'autres éléments formant la nouvelle pierre apparaissent – ils ont la même topologie, mais des propriétés et un chargement différents. Enfin, le transfert d'effort de la structure vers la nouvelle unité, ce que l'on peut appeler la réactivation, est complexe à modéliser correctement. A cet effet, deux modèles sont proposés. L'un, homogène, décrit le procédé global de remplacement. L'autre, qui prend en compte la mésostructure de la maçonnerie, est plus adapté pour décrire le phénomène de réactivation.

Une surface représentative de l'arc le plus endommagé est étudiée à l'aide d'une analyse linéaire aux éléments finis, et les facteurs les plus influents sont déterminés. Le critère visé est la minimisation de la déformation de l'arc et de l'augmentation locale de contrainte dans les pierres alentours.

**Mots clef :** maçonnerie traditionnelle de pierre, patrimoine historique, Éléments Finis, techniques de restauration, méthodes de construction par phases



# Contents

<b>Thesis proposal</b>	<b>i</b>
<b>Declaration</b>	<b>iii</b>
<b>Acknowledgements</b>	<b>v</b>
<b>Abstract</b>	<b>vii</b>
<b>Table of contents</b>	<b>xi</b>
<b>List of figures</b>	<b>xiii</b>
<b>List of tables</b>	<b>xviii</b>
<b>Introduction</b>	<b>1</b>
<b>1 The Charles Bridge</b>	<b>5</b>
1.1 History . . . . .	5
1.2 Intervention . . . . .	6
1.3 Fourteenth arch investigation . . . . .	10
1.3.1 Description of the arch . . . . .	10
1.3.2 Material . . . . .	10
1.3.3 State of the arch . . . . .	11
<b>2 Modeling of the intrados</b>	<b>19</b>
2.1 Introduction to the problem . . . . .	19
2.1.1 General considerations . . . . .	19
2.1.2 Description of the site process of replacement . . . . .	20
2.2 Modeling of masonry . . . . .	21
2.2.1 The material . . . . .	21

2.2.2	Modeling approaches . . . . .	22
2.3	FEM method and OOFEM software . . . . .	23
2.3.1	The Finite Element Method (FEM) . . . . .	23
2.3.2	OOFEM software . . . . .	23
2.4	Hypothesis of the model . . . . .	24
2.4.1	Geometry of the section . . . . .	24
2.4.2	Two models . . . . .	25
2.4.3	Type of elements . . . . .	25
2.4.4	Material . . . . .	25
2.4.5	Loading . . . . .	27
2.4.6	Boundary conditions . . . . .	27
2.5	Presentation of the results . . . . .	29
<b>3</b>	<b>Homogeneous model</b>	<b>31</b>
3.1	Description . . . . .	31
3.1.1	General idea . . . . .	31
3.1.2	Creating the computational model . . . . .	31
3.1.3	Modeling the new stone activation . . . . .	33
3.2	Model of the reduced area of the arch . . . . .	37
3.2.1	Replacement of one column . . . . .	37
3.2.2	Replacement of one row . . . . .	39
3.2.3	Replacement of 4 columns . . . . .	41
3.3	Discussion on the model . . . . .	44
3.3.1	Capabilities of the model . . . . .	44
3.3.2	Limits of the model . . . . .	44
<b>4</b>	<b>Heterogeneous model</b>	<b>47</b>
4.1	Description . . . . .	47
4.1.1	Creating the computational model . . . . .	47
4.1.2	Modeling the new stone activation . . . . .	50

---

4.1.3	Influence of the location of the stone . . . . .	58
4.1.4	Influence of the size of the stone . . . . .	60
4.1.5	Consequences of the linearity of the model . . . . .	61
4.1.6	Importance of the activation process . . . . .	66
4.2	Application to the reduced area of arch . . . . .	68
4.3	Limits of the model . . . . .	70
	<b>Conclusion</b>	<b>71</b>
	<b>References</b>	<b>77</b>





# List of Figures

1.1	The Charles Bridge, Prague 1 . . . . .	5
1.2	Location of the Charles Bridge over the Vltava River . . . . .	6
1.3	History of the Charles Bridge . . . . .	7
1.4	Section of the arch 14 . . . . .	10
1.5	Location of the drill core for destructive testing in laboratory . . . . .	12
1.6	Current scaffolding on the 14th arch . . . . .	13
1.7	Material of the part of the arch joining pillar 13 . . . . .	14
1.8	Material of the part of the arch joining pillar 14 . . . . .	15
1.9	Legends of the cartographies . . . . .	16
1.10	Damaged state of the part of the arch joining pillar 13 . . . . .	17
1.11	Damaged state of the part of the arch joining pillar 14 . . . . .	18
2.1	Masonry behavior [11] . . . . .	21
2.2	Modeling strategies for masonry structures: (a) masonry sample; (b) detailed micro-modeling; (c) simplified micro-modeling; (d) macro-modeling [13] . . . . .	22
2.3	Reduced area of the arch chosen for the study . . . . .	26
2.4	Boundary conditions applied to the section . . . . .	28
3.1	Flowchart of the homogeneous model . . . . .	32
3.2	Geometry and mesh of the reduced area implemented in the homogeneous model . . . . .	32
3.3	Plane stress element used for the homogeneous model . . . . .	33
3.4	Distribution of $\sigma_{yy}$ [MPa] caused by uniform eigenstrain loading of the inserted stone . . . . .	34

3.5	Revised flowchart of the homogeneous model . . . . .	35
3.6	Non uniform distribution of eigenstrain to activate the new stone, applied to vertical sections multiple of 1/6 of the stone width . . . . .	36
3.7	Distribution of $\sigma_{yy}$ [MPa] caused by piecewise eigenstrain loading of the inserted stone	36
3.8	Vertical displacement [m] in the homogeneous model when restoring 1 column (deformed shape $\times 2000$ ) . . . . .	37
3.9	Distribution of $\sigma_{yy}$ [MPa] in the homogeneous model when restoring 1 column (deformed shape $\times 2000$ ) . . . . .	38
3.10	Vertical deformation [m] in the homogeneous model in time when restoring 1 column .	38
3.11	Vertical displacement [m] in the homogeneous model when restoring 1 row (deformed shape $\times 2000$ ) . . . . .	39
3.12	Distribution of $\sigma_{yy}$ [MPa] in the homogeneous model when restoring 1 row (deformed shape $\times 2000$ ) . . . . .	40
3.13	Vertical deformation [m] in the homogeneous model in time when restoring 1 row . . .	40
3.14	Vertical deformation [m] in the homogeneous model in time when restoring the reduced area column by column in 4 stages . . . . .	41
3.15	Vertical displacement [m] in the homogeneous model when restoring 4 columns (deformed shape $\times 3000$ ) . . . . .	42
3.16	Distribution of $\sigma_{yy}$ [MPa] in the homogeneous model when restoring 4 columns (deformed shape $\times 3000$ ) . . . . .	43
4.1	Flowchart of the heterogeneous model . . . . .	48
4.2	Geometry and mesh of the reduced area implemented in the heterogeneous model . . .	48
4.3	Zoom of the modeling of one stone and surrounding mortar of the heterogeneous model	49
4.4	Plane stress element used for the heterogeneous . . . . .	49
4.5	Process of activation of the new stone for the heterogeneous model . . . . .	50
4.6	$\sigma_{yy}$ distribution [MPa] in the heterogeneous $\sigma_{yy}$ model when restoring 1 stone . . . . .	51
4.7	Vertical displacement [m] in the heterogeneous model when restoring 1 stone (deformed shape scale $\times 1000$ ) . . . . .	52

4.8	Final $\sigma_{yy}$ distribution [MPa] in the heterogeneous model when removing one stone . . .	53
4.9	Final vertical displacement [m] in the heterogeneous model when restoring 1 stone (deformed shape scale $\times 1000$ ) . . . . .	53
4.10	Vertical displacement [m] in the heterogeneous model for different time steps (de- formed shape scale $\times 2000$ ) . . . . .	54
4.11	$\sigma_{yy}$ distribution [MPa] in the heterogeneous model for different time steps (deformed shape scale $\times 3000$ ) . . . . .	54
4.12	Shear stress $\tau_{xy}$ [MPa] in the heterogeneous model for different time steps (deformed shape scale $\times 2000$ ) . . . . .	55
4.13	Behavior of the heterogeneous model during the replacement process . . . . .	55
4.14	$\sigma_{yy}$ stress distribution in the heterogeneous model for different time steps . . . . .	56
4.15	Vertical deformation of the heterogeneous model when restoring 5 different stones . . .	58
4.16	Increase in vertical deformation compared to the deformation due to the replacement of the middle stone 16 . . . . .	59
4.17	Path of the loads when the stone is removed for different procedures of replacement of the stones . . . . .	60
4.18	3D plot of the deformation of the heterogeneous model for different activation pressures and different sizes of stone (red: $p = 0$ MPa, blue: $p = 0.18$ MPa, green: $p = 0.36$ MPa, yellow: $p = 0.5$ MPa) . . . . .	60
4.19	Vertical deformation of the heterogeneous model [ $\times 10^{-6}$ ] for different values of acti- vation pressure and different dimensions of stone (numerical points are marked in black)	62
4.20	Deformation of the heterogeneous model for different activation pressures and different dimensions . . . . .	63
4.21	State of stress [MPa] for the two extreme widths of a stone examined (0.7 m high) . . .	64
4.22	Comparison of the behavior of the heterogeneous model when using 4 stages in one model or 4 models of 1 stage . . . . .	65
4.23	Comparison of the behavior of the heterogeneous model when using 4 stages in a model, 4 models of 1 stage, and the sum of the results of the previous 4 models . . . .	66

4.24	Vertical deformation of the heterogeneous model for different activation pressures when using 4 stages in a model, 4 models of 1 stage, and the sum of the results of the previous 4 models . . . . .	67
4.25	Vertical deformation of the examined reduced area in time . . . . .	68
4.26	Vertical deformation [m] of the examined reduced area . . . . .	69
4.27	$\sigma_{yy}$ stress [MPa] in the examined reduced area . . . . .	69

# List of Tables

1.1	Main floods and maintaining operations on the Charles Bridge [25] [26] . . . . .	8
1.2	Characteristics of the material of the arch . . . . .	11
2.1	Mechanical characteristics of the materials . . . . .	27
4.1	Comparison of the deformation in the heterogeneous model when using 4 stages in a model, 4 models of 1 stage, and the sum of the results of the previous 4 models . . . .	67



# Introduction

## Motivation

The Charles Bridge is part of the world heritage: such piece of Gothic architecture must be maintained as a remain of history. Urgent attention should be paid to the intrados of the arches, where the masonry exhibits advanced state of weathering. Maintaining historical masonry is a delicate work. Usually, the technique of patching is used: the damaged surface of stone units is removed, and replaced with new elements of compatible stone, bonded to the old part with traditional mortar. Nonetheless, in the case of the actual structure, the weathering jeopardizes the mechanical properties of the stone. Therefore, some units should be entirely changed.

When important intervention is done on historical building, the motivations for it must be justified, as well as the low impact of the intervention – both when work is in progress and in the final state. Structural analysis of the structure based on a computational model is often carried out. Combined with site investigation, the computational model is used to understand the current state of the structure according to its loading history. It also enables to prepare the intervention and to predict its consequences. Finally, it is a valuable tool for the maintenance after the intervention.

To prepare the restoration of the intrados of the Charles Bridge, a computational model is required to minimize the impact of the replacement of weathered stones on the global deformation of the arch and, locally, on the increase of stress or the development of tensile stress around the stone. The methodology would be used by engineers to design and validate the stages of replacement.

## Objectives

This thesis focuses on the development and discussion of a methodology to model the replacement stage by stage of some damaged stones of the intrados of the Charles Bridge in Prague.

Modeling strategy should be established to study the arches of the bridge, based on linear finite element analysis. Two points should be treated with particular attention. First, the mod-

eling of different stages, with, for each stage, changes in the static scheme and in the properties of the elements that constitutes the replaced stone. Then, the modeling of the reactivation of the newly inserted stone, to describe the transfer of loads from the structure to the new block.

This computational model would then be a tool to determine the best replacement procedure to minimize global deformation of the arch and prevent local increase of stress and development of tensile stress.

## **Outline**

First, a brief presentation of the history of the Charles Bridge and its current state enables to understand the structure and its needs for restoration. Then, a first model is proposed: it is homogeneous, and can only describe the impact of the replacement of weathered stones on the global deformation. For this reason, a second model is created: it takes into account the mesostructure of masonry and is more suitable to describe the phenomenon of reactivation of the newly inserted stone and to capture local increase of stress. Those two methodologies are discussed and compared in order to cover all the requirements of modeling for the restoration of the intrados.







# Chapter 1

## The Charles Bridge



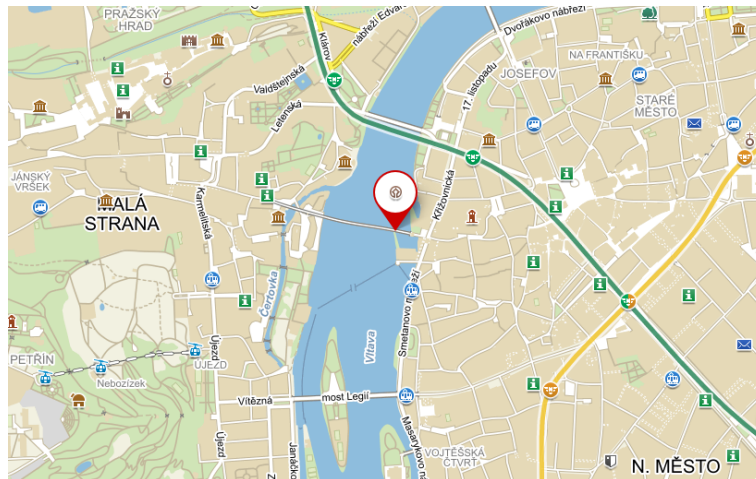
**Figure 1.1:** The Charles Bridge, Prague 1

### 1.1 History

The Charles Bridge (Karlův Most, Figure 1.1) is one of the most important monuments of the city of Prague. It is classified in the National Historic Monuments list and by UNESCO Committee. It was built between 1357 and 1406, when Charles IV was king of Bohemia, Germany, Italy, and the Holy Roman Empire [26]. The legend reports that the king laid the first stone 5:31am on 9 July 1357, which would give the construction great strength according to numerology beliefs (1357 9, 7 5:31). He entrusted Petr Parléř the charge to design and build the

bridge.

The bridge links the two historical areas of Malá Strana and Nové Město over the Vltava River, the main river crossing the city of Prague (see figure 1.2). It replaced the Judith Bridge that collapsed in 1273 due to several floods (see figure 1.3a). As it was on a strategic trade road through Eastern Europe, a wooden bridge was built quickly, that was later replaced by this monumental stone bridge.

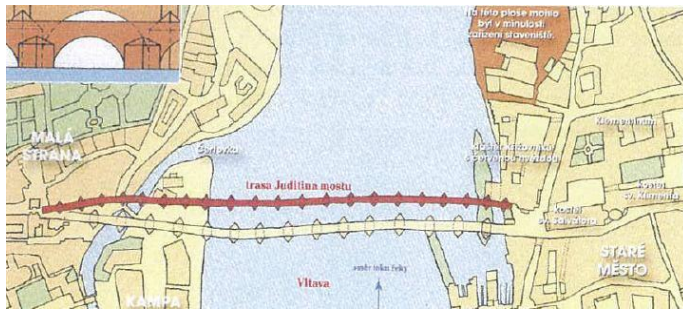


**Figure 1.2:** Location of the Charles Bridge over the Vltava River

The construction of the Charles Bridge represented a challenge in its time (see figure 1.3b). The bridge is 515.76 m long, the spans between two pillars are between 16.62 m and 23.38 m. The width of the deck is 10 m. It is composed of 16 arches. On the bridge parapet are several baroque sculptures, all representing saints or scenes from the Bible. On the river banks stand two watchtowers, another emblems of the city. The construction was first supposed to support the merchant caravans crossing the city. Later, the bridge was adapted for trams and buses. Nowadays, it is only pedestrian so the loads have reduced a lot through times.

## 1.2 Intervention

Since the Charles Bridge was the main and only way to cross the Vltava river in a perimeter of 100 km around Prague during a long time, it was maintained in a good state. Nowadays, its cultural patrimony is the reason for maintenance since other bridges were built in the city.



(a) Location of the old Judith Bridge



(b) Construction of the Charles Bridge

**Figure 1.3:** History of the Charles Bridge

The main causes for the deterioration of the state of the bridge are:

- self weight
- weathering (wind, erosion of the water, aggressive salts...)
- floods
- thaw and frost cycles (there can be an annual variation of temperature of 40 °C [2])
- movement of foundations

The flood episodes, some very damaging, are compiled in the Table 1.1. Some parts of the bridge collapsed due to floods, and pillars were as well severely damaged. Floods can cause angular rotation, subsidence, and shift on a bridge pillar. They cause tensile stress in the arches, which leads to local damage of the masonry.

From 1966 to 1975, an important restoration work was started. However, this intervention was afterwards highly criticized because cement mortar was used instead of traditional materials. The deck was strengthened with a reinforced concrete slab and hydro-insulation was installed. It is also the time when the bridge was closed to vehicles in order to preserve it [26]. Concerning the stones, the technique of patching was used: only a superficial part of the brick was replaced with new stone and bonded to the remaining part with cement. Though this method is advised, rather than replacing the whole block when it is possible, it requires compatible properties of stone and mortar, which was not the case for the Charles Bridge. Later, the patches turned into

Table 1.1: Main floods and maintaining operations on the Charles Bridge [25] [26]

Year	Event	Cause
1357	First stone is laid	
1406	Completion of the works	
1432	Damage to piers No. 3, 4, 7, 8, 10	Flood
1496	Collapse of two arches (No. 3 and No. 4) and one pillar (No. 3) already eroded	Heavy load on eroded pillar
till 1503	Repair of damage from years 1432 and 1496	
1648	Old Town Bridge Tower damaged by Swedes	Thirty Years' War
1655	Damage to pier foundations	Flood
1784	Partial damage to the foundation of three piers and five vaults	Flood
till 1788	Repair of damage from year 1784	
1844	Replacement of the stairway to Kampa Island	
1866	Placement of pseudo-Gothic gas lights	
1870s	Bridge become way for public transports	
1874–1883	Reconstruction of the Bridge Towers	
1890	Vaults No. 5, 6 and 7 destroyed, piers No. 4, 8 damaged	Flood
1893	Repair of damage from year 1890	
1903	Rehabilitation of piers No. 3, 4 and 7 (Velflik arches)	
1905–1912	Replacement works (with Horice sandstone) on facing masonry of piers No. 1, 2, 8, 11 and 12 and neighbouring arches	Use of low durability stone
1926–1928	Replacement works (with Horice sandstone) on facing masonry of piers No. 4, 5, 9 and 10 and neighbouring arches	Use of low durability stone
1966–1975	Major reconstruction, grouting, water-proofing layer, stabilising reinforced concrete slab installed, replacement of facing masonry; it is pedestrianized	Use of Portland cement based mortar as binder
1980s	Additional localized replacements	Cement mortar
1994–1997	Study leading to the undone large-scale repair	
2002	More than 100-year flood, the bridge survived	
2004–2005	Strengthening of foundations (piers No. 8 and No. 9)	
2007–2010	Repair of parapets, dilatation joints, hydro-isolation of the pavement, rehabilitation of foundations, gas lighting	

odd colors (beige to yellow) [22], and some parts of the arch did not behave as massive masonry: the bricks were not interdependent anymore. The development of biochemical decay in the layer between the old stone and the new patches fostered the global damage of the bridge. This intervention is one of the explanation for the advanced degradation of certain stones of the arches.

Another important intervention took place in 1990, to assure the overall stability of the bridge and its bearing capacity. This time, a multiscale approach was considered, in order to

treat both local problems and their consequence on the global behavior.[26]

The final intervention occurred from 2007 to 2010. It aimed at the rehabilitation of the foundations as well as the hydro-insulation of the pavement on the deck. Some smaller works were done at that time (repair of the parapet, renewal of gas lighting). This very recent intervention was the opportunity to install a monitoring system to control the temperature and the moisture content [12], and an to create an information database (<http://iskarluvmost.fsv.cvut.cz/>).

From then on, no major operation was done on the bridge. However, the development of more and more powerful numerical tools enabled to have a better knowledge of the behavior of the bridge through several research programs and modeling campaigns at the Czech Technical University. However, some parts of the Charles Bridge present a concerning state.

## 1.3 Fourteenth arch investigation

### 1.3.1 Description of the arch

The most damaged arch is the 14th one. The company Pudis [7] was in charge of the site investigation of the arch.

The 14th arch is partly above the river bank, and partly above the Čertovka, a small arm of the Vltava. The arch is made of several layers of stone masonry. The first layer is thick 450 mm and is made of very good ashlar masonry, put vertically, followed by a layer of horizontal stones. A final layer of vertical stones stiffens the arch before the beginning of the masonry deck. Between the two lateral masonry walls, on top of the arch, is the infill made of rubble masonry bonded with very good mortar (see Figure 1.4).

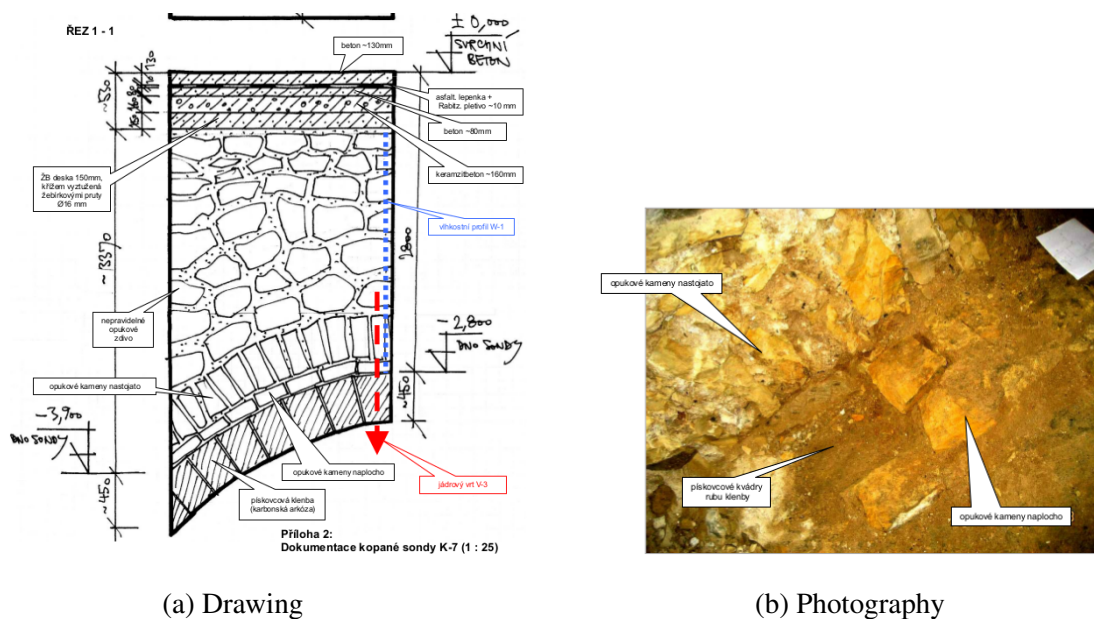


Figure 1.4: Section of the arch 14

### 1.3.2 Material

The Charles Bridge is made of stone masonry. The stones have good properties, and their disposition shows that it is a high quality masonry, with well cut ashlars and thin layers of good



mortar. This is due to the fact that the bridge was a key passage through Eastern Europe during centuries and was ordered by Charles IV who also used it as a symbol of his power.

The inspection of the arch enabled to establish a cartography of the arch. Due to repairs through history, different stones can be found (see Figures 1.7 and 1.8). The values of the material mechanical characteristics are summarized in the table 1.2.

Table 1.2: Characteristics of the material of the arch

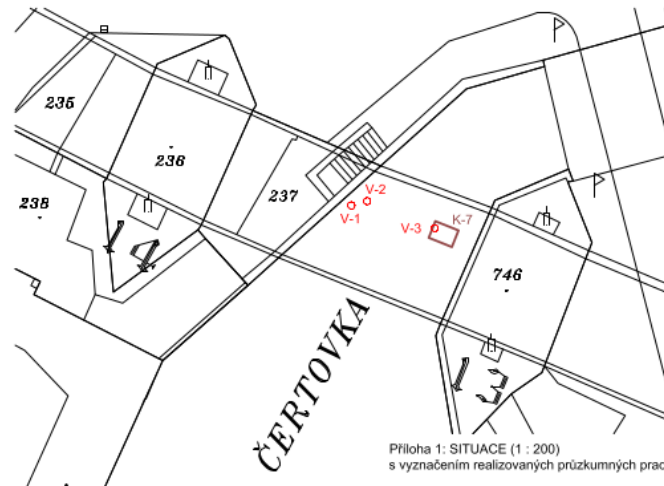
	units	extreme values	mean value
<b>original sandstone</b>			
density	kg/m <sup>3</sup>	1963 - 2100	2023
compressive strength (on rollers)	MPa	7.3 - 13.1	9
compressive strength (hardness)	MPa	7.2 - 12.5	9.9
classification		ČSN 73 1001 4	
<b>sandstone of the repair patches</b>			
compressive strength (hardness)	MPa	27.7 - 35.3	30.5
classification		ČSN 73 1001 R3	
<b>marl of the infill</b>			
compressive strength	MPa	20.1 - 49.6	30.8
classification		ČSN 73 1001 R3	
<b>mortar of the infill</b>			
compressive strength	MPa	6.5 - 14.4	10.9
<b>mortar between original blocks</b>			
compressive strength	MPa	1.6 - 2.5	2
<b>mortar between rhabilited blocks</b>			
compressive strength	MPa	6.1 - 9.3	7.7
<b>irregular masonry of the infill</b>			
density	kg/m <sup>3</sup>	1902 - 1946	1931
compressive strength (on rollers)	MPa	8.7 - 9.6	9.2
<b>Conclusion</b>			
original stone compressive strength	MPa		10
repair patches compressive strength	MPa		30
irregular infill compressive strength	MPa		30
mortar between original blocks	MPa	1.5 - 2.5	
repair blocks	MPa		6 - 9

### 1.3.3 State of the arch

#### 1.3.3.1 Site investigation

The following both destructive and non destructive methods were used to estimate the state of the masonry:

- Visual inspection that led to establish a cartography (see Figures 1.11 and 1.11).
- Samples were extracted in some areas (see Figure 1.5).
  - two vertical drills of 90 mm at the crown of the arch



**Figure 1.5:** Location of the drill core for destructive testing in laboratory

- one sample at the foot of the arch (K7)
  - 3 inclined upward drills of 50 mm of diameter and 500 – 600 mm long into selected sandstone blocks to determine the way of their previous repair how they were repaired
  - 1 vertical core drill (V-3) from the bottom of (K7)
- Tests in compression were executed on the sandstone samples in order to get information on the mechanical properties (Young modulus, compressive strength).
  - Tests in concentrated compression were executed on irregular specimens of marlstone.
  - The Schmidt rebound hammer was used to determine qualitatively the compressive strength. However, this non destructive method is not reliable for quantitative values, especially in our case where the stone is might differ from one block to another.
  - The so called local violation method (Ing. Kučera, CSc., TZÚS Prague [7]) was used to determine the strength of the joint mortar.

### 1.3.3.2 State of damage

From the cartographies (see Figures 1.11 and 1.11), one can distinguish four states of stones. The green ones are in a good state. The white ones, which represent the biggest surface, are



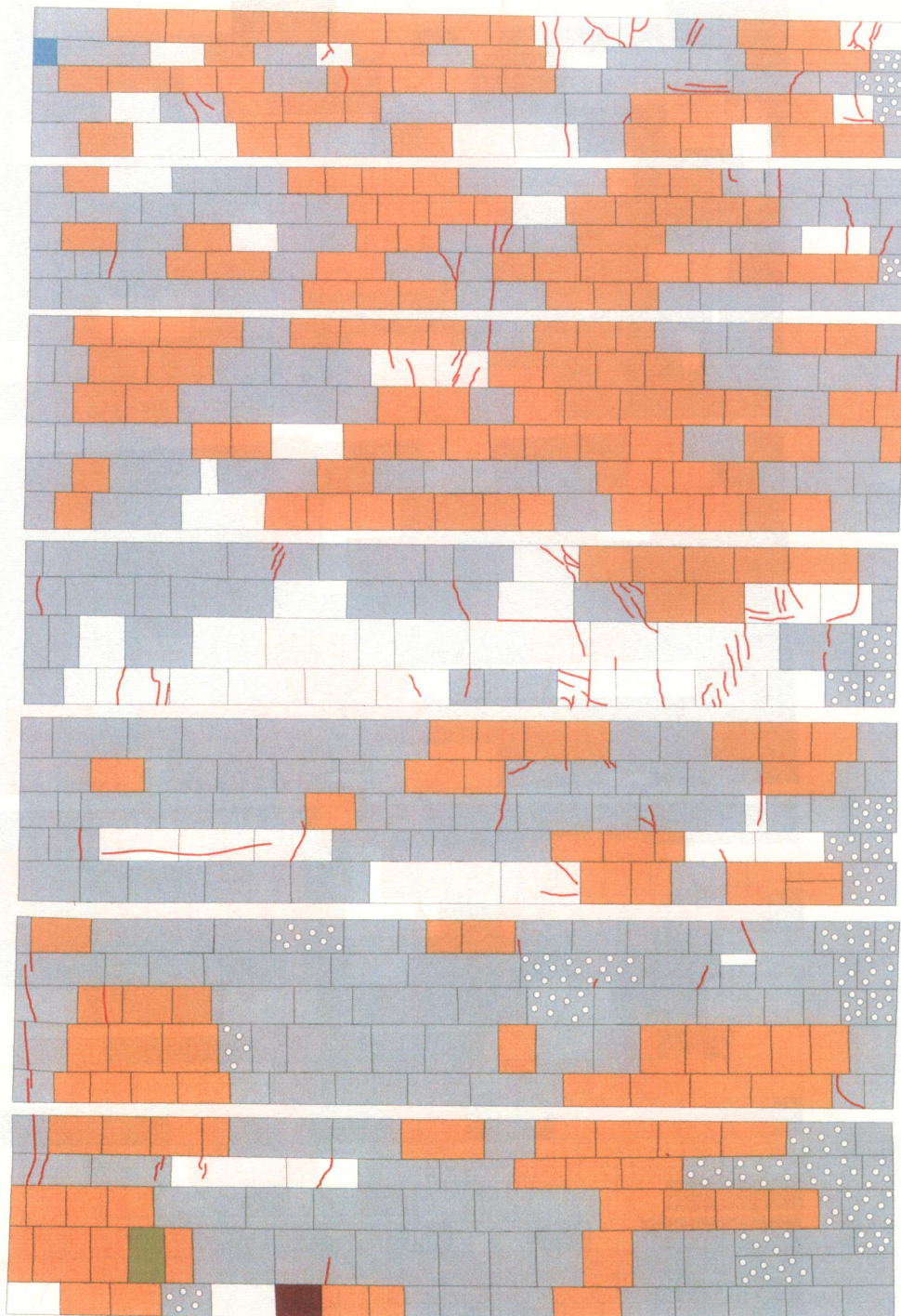
**Figure 1.6:** Current scaffolding on the 14th arch

slightly weathered and shall be inspected every 5 years. The yellow ones are even more concerning. Finally, the red ones, which represent 15% to 20% of the total surface, are in an advanced damaged state and should be replaced as soon as possible. They can be found all over the surface. However, they are especially concentrated at the bottom of the arch, where is the rising damp, as well as at the top, at the connection with the deck. The red stones are the ones that this study first targets.

Currently, the arch is sustained with wooden scaffolding and fabric material to avoid pieces of stone falling (see Figure 1.6). It was a necessary intervention in order to maintain the arch before any further repair is possible.

Podrobný materiálový průzkum kamenného kvádřového zdiva Karlova mostu	Výsledky v úsecích kleneb a poprsních zdí polí XIV, XV a XVI a pilířů 13, 14 a 15	Objednáno: Mott Mac Donald Praha s.r.o. Smlouva: 90-907457
---	---	--

## Klenba XIV, úsek č. 13, východní část



(zde navazuje na pilíř č. 13)


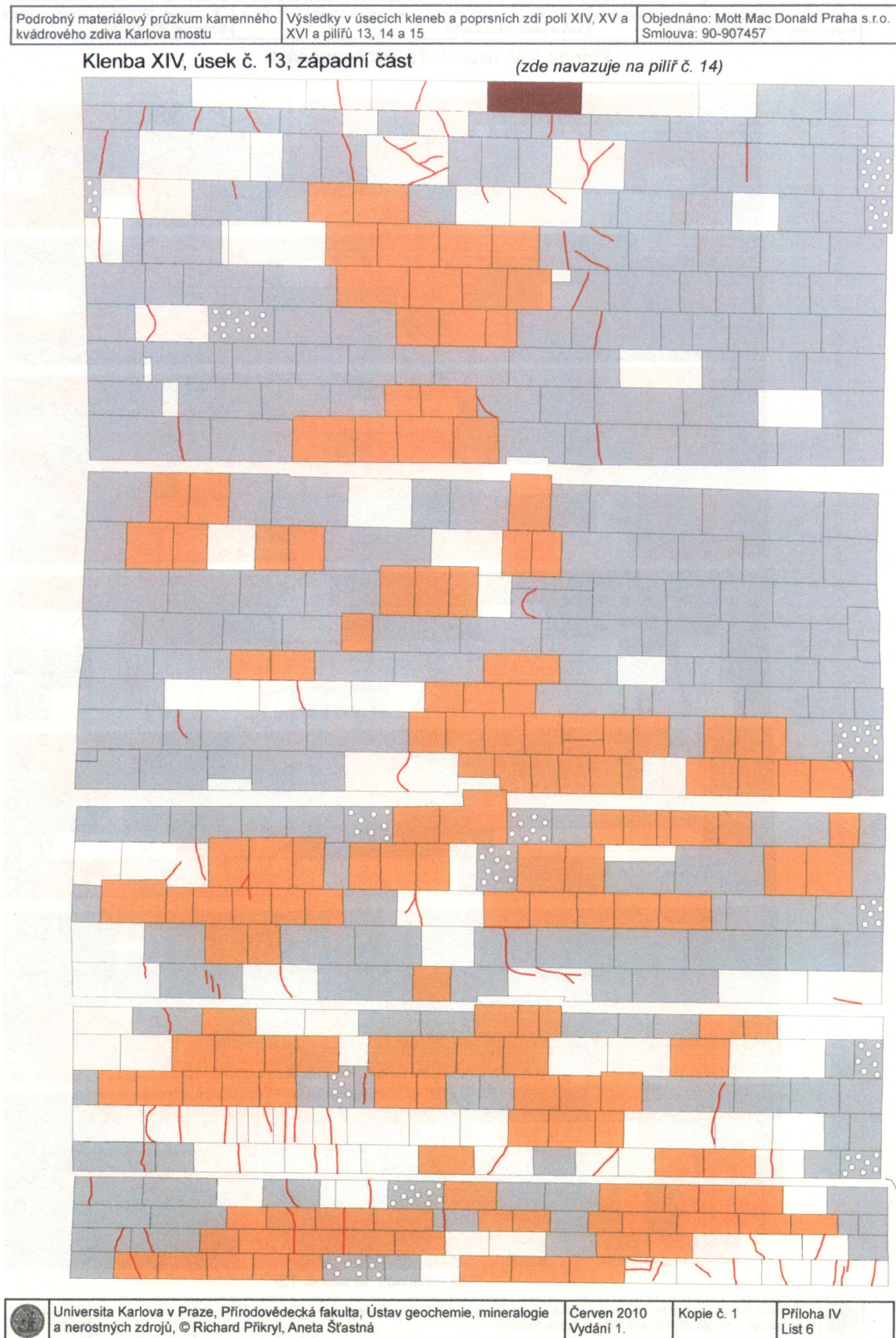
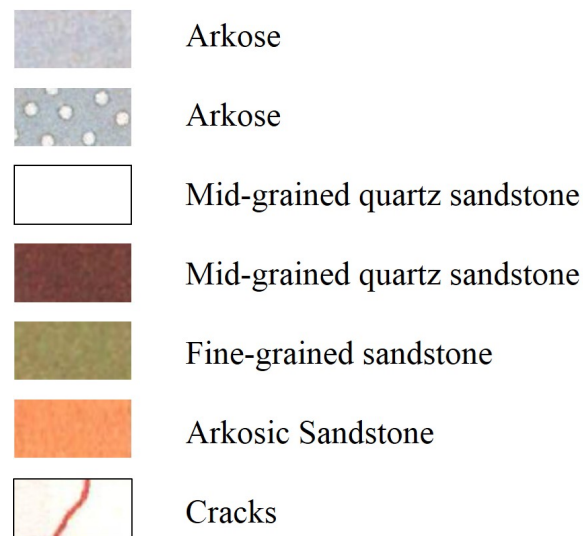
 Universita Karlova v Praze, Přírodovědecká fakulta, Ústav geochemie, mineralogie a nerostných zdrojů, © Richard Píkrýl, Aneta Štátná	Červen 2010 Vydání 1.	Kopie č. 1	Příloha IV List 5
--	--------------------------	------------	----------------------

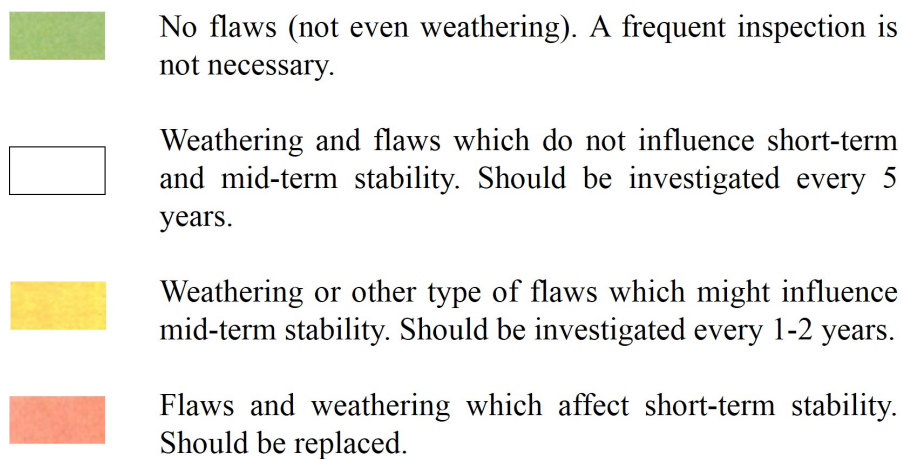
Figure 1.7: Material of the part of the arch joining pillar 13



**Figure 1.8:** Material of the part of the arch joining pillar 14

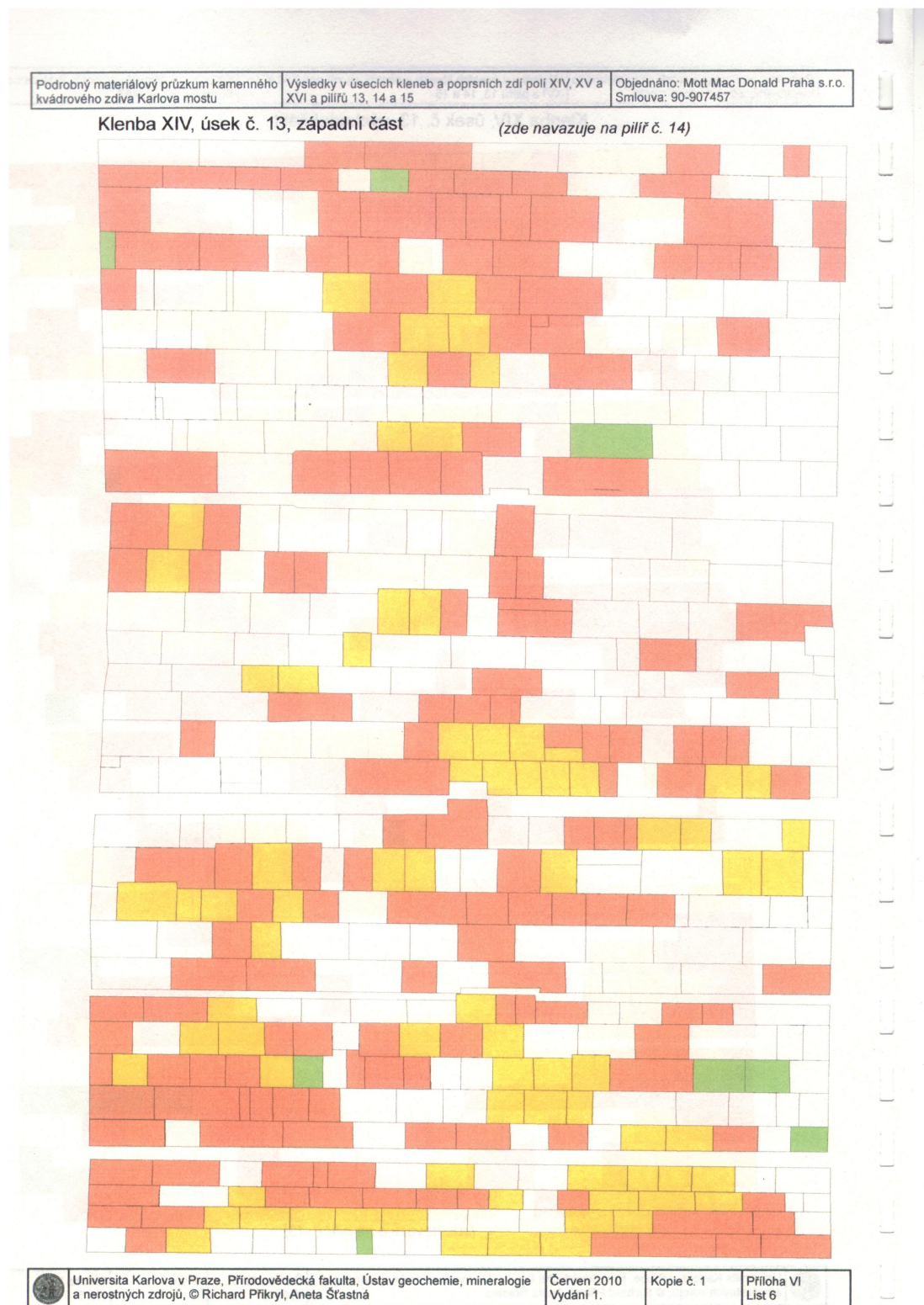


(a) Legend of the material cartography



(b) Legend of the state cartography

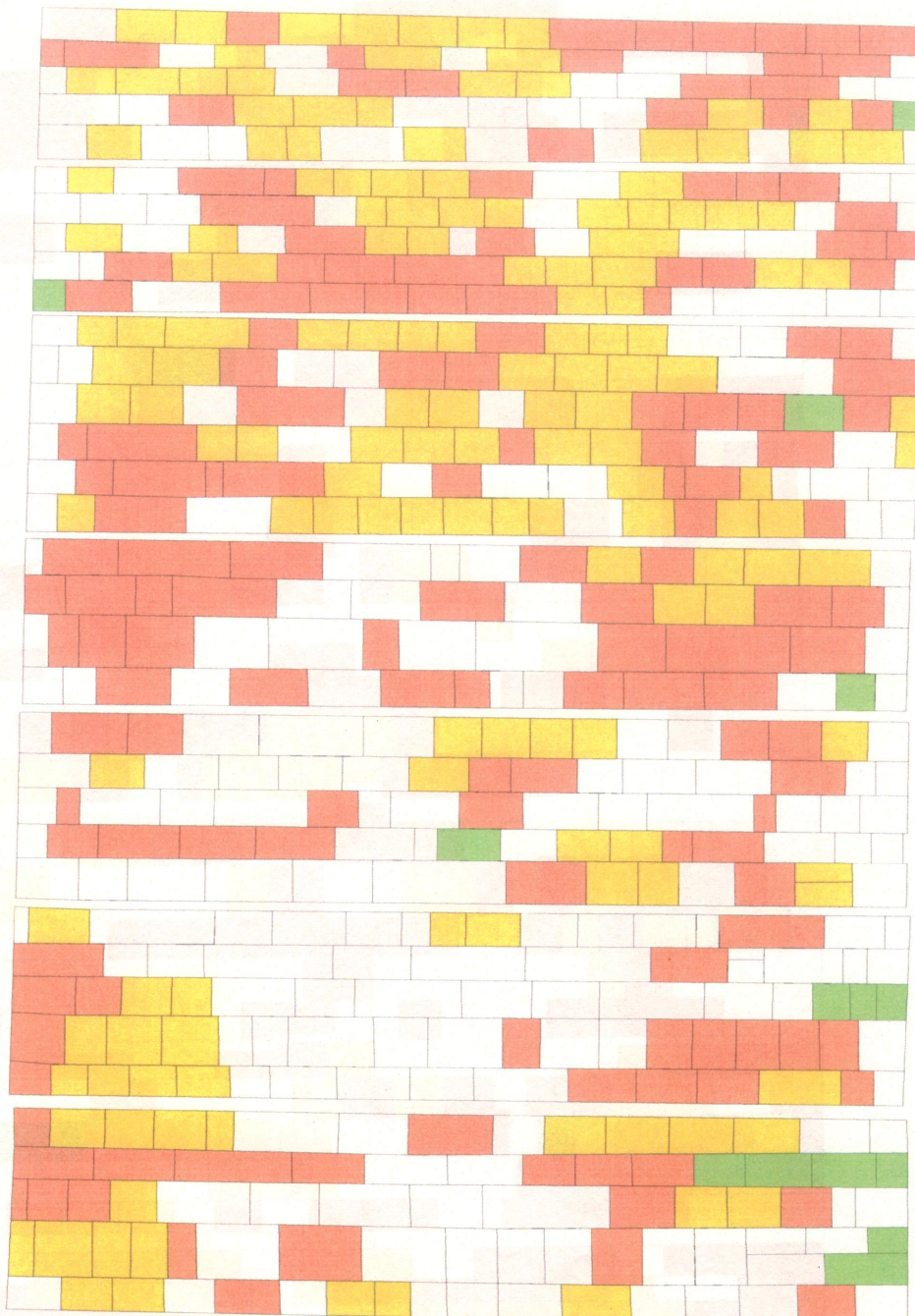
**Figure 1.9:** Legends of the cartographies



**Figure 1.10:** Damaged state of the part of the arch joining pillar 13

Podrobný materiálový průzkum kamenného kvádřového zdiva Karlova mostu	Výsledky v úsecích kleneb a poprsních zdí polí XIV, XV a XVI a pilířů 13, 14 a 15	Objednáno: Mott Mac Donald Praha s.r.o. Smlouva: 90-907457
---	---	---

## Klenba XIV, úsek č. 13, východní část



(zde navazuje na pilíř č. 13)


 Universita Karlova v Praze, Přírodovědecká fakulta, Ústav geochemie, mineralogie a nerostných zdrojů, © Richard Příkryl, Aneta Šťastná	Červen 2010 Vydání 1.	Kopie č. 1	Příloha VI List 5
--	--------------------------	------------	----------------------

Figure 1.11: Damaged state of the part of the arch joining pillar 14



# Chapter 2

## Modeling of the intrados

### 2.1 Introduction to the problem

#### 2.1.1 General considerations

The following work tries to find a suitable numerical approach in order to optimize the replacement of some specific highly damaged stones of the arches of the Charles Bridge. The 14th arch is taken as an example since it is the most damaged one. There are two main tracks to develop and to achieve it. First, a numerical model that can capture the global behavior of the arch of the bridge and the local consequences around the replaced stones needs to be developed. Then, based on the results, and with the aim of reaching a reasonable time of the reconstruction and minimizing additional damage to the bridge or to adjacent stones, general recommendations could be drawn. This thesis focuses on the first part of the problematic that consists in the building of a computational model.

The two main criteria of the study are therefore:

- The global vertical deformation of the arch due to the axial shortening of the arch when a stone is removed.
- The increase in local stress concentration that may deteriorate the integrity and good mechanical properties of the surrounding stones.

The present study does not concern the ultimate state or the stability of the arch and will not consider damage mechanics of the stones or of the structure. The restoration of the bridge must not affect the structure beyond serviceability state.

One of the main difficulties of this work is that there is no similar question academically treated before. All that can be found concerns the chemical and mechanical compatibility of the new pieces of stone. For this reason, the work is done incrementally, to improve step by step the modeling of the physical phenomena, and results in two different models.

### **2.1.2 Description of the site process of replacement**

One of the main steps of the modeling was the activation of the new stone: how to transfer the stress from the remaining adjacent stones to the new piece? To answer this question, it is first necessary to understand the site process. However, there are few written records about historical mason skills. This is why it should be necessary for a more detailed study to contact a company dealing with historical techniques.

When restoring masonry elements, the smallest quantity of material as possible should be removed. In the current case of weathered stones, the widest spread technique, called patching, consists in removing only the damaged surface and refilling with a thin layer of new stone. Nonetheless, this solution is suitable when the weathering is superficial. In the current case, stones have to be removed. If it is possible, the surrounding area should not be dismantled [9]. The mortar is gently taken off around the damaged stone to release it, and the dust in the hole is cleaned up. Then the prepared ashlar stone is placed in the hole. Some wooden edges are installed on the top of the stone and driven in until the appropriate stress in the new stone is reached. Finally, a fresh mortar is applied all around the block. When the mortar is strong and stiff enough to transfer the stress, the wooden wedges are released. An interesting picture to understand this process is to imagine prestressed stone: the presence of wooden wedges enables to prestress the stone unit.

The question of the compatibility of the new unit compared to the masonry in place is very important. Both the chemical composition and the mechanical properties should be close to the adjacent stones [8]. However, this question is not treated here.

## 2.2 Modeling of masonry

### 2.2.1 The material

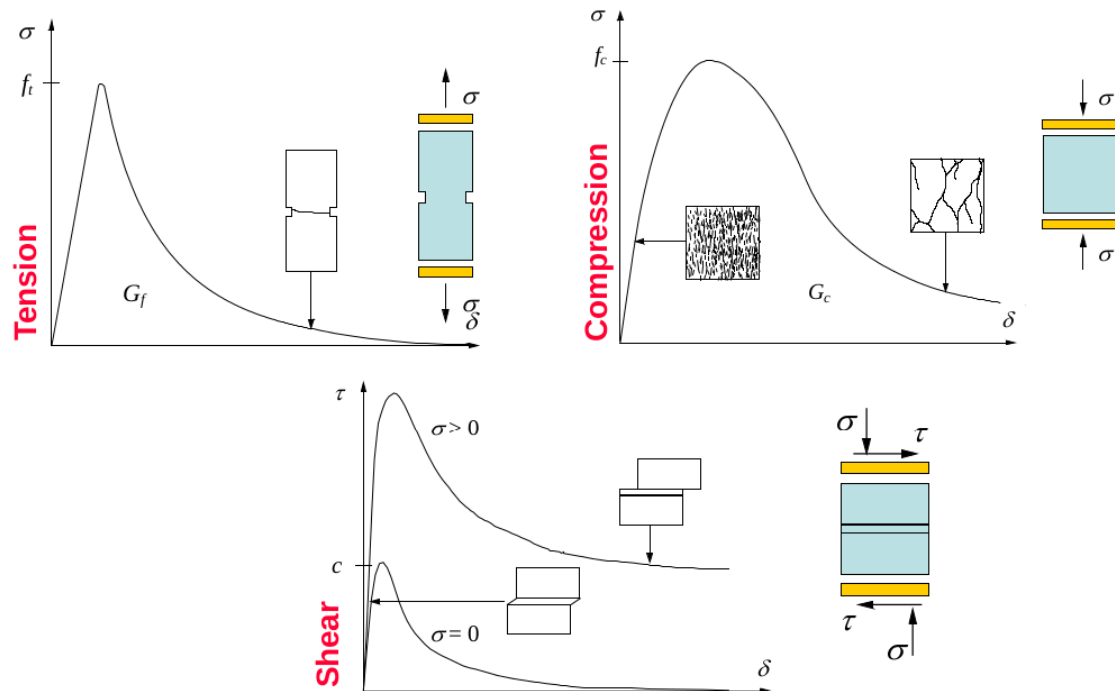


Figure 2.1: Masonry behavior [11]

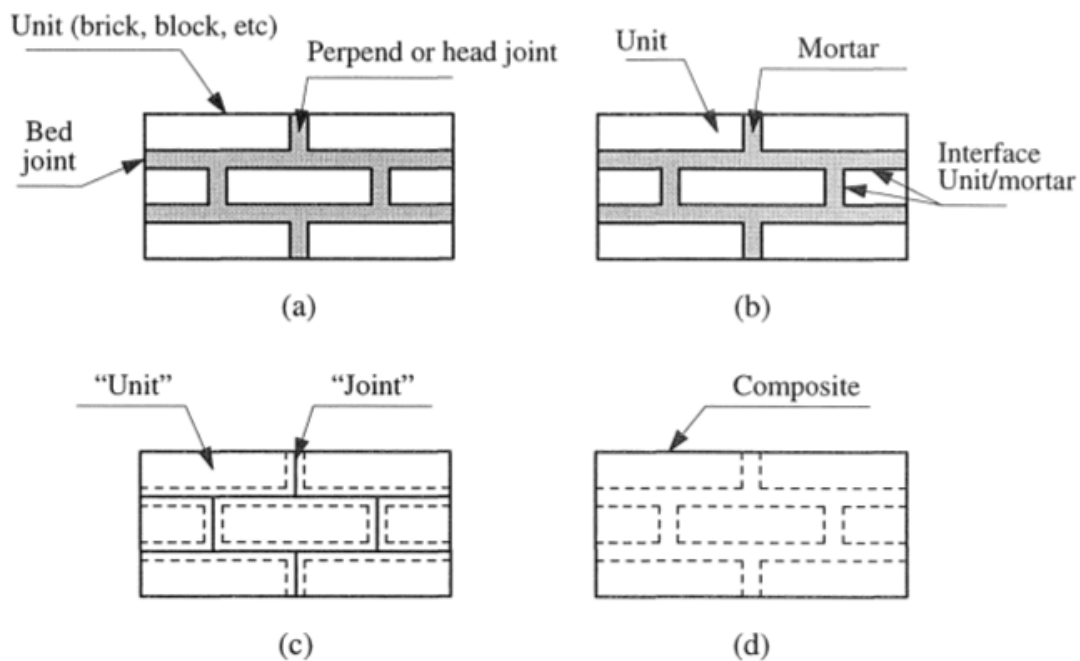
Masonry is an anisotropic material because it is a composite made of stone units and mortar joints. Multiscale modeling is therefore required. The great variability in the mechanical properties and in the geometry from one type of masonry to another makes each modeling approach a unique problem. In the specific case of historical masonry, the different interventions through times are another source of complexity since different materials and techniques can be spotted in one structural element.

The global properties depend on the properties of the mortar joints, of the stone units, and on the bond between them. Masonry has good properties in compression. It has a brittle response in tension (very low tensile strength, around 10% of the compressive strength), and a frictional response in shear (once the limited bond between units and mortar is lost) (see Figure 2.1).

## 2.2.2 Modeling approaches

There are two main approaches to model masonry [13] (see Figure 2.2).

- *Micro-modeling*: the bricks and the mortar are two different materials, with their own mechanical properties. The layers of mortar have a non-zero thickness and are linked to the brick units by interface elements.
- *Macro-modeling*: masonry is considered as a continuous material with its own properties, that are neither the mortar properties, nor the stone ones. The determination of these properties rely on homogenization of the individual properties [14]. This solution is often used for large scale structures.



**Figure 2.2:** Modeling strategies for masonry structures: (a) masonry sample; (b) detailed micro-modeling; (c) simplified micro-modeling; (d) macro-modeling [13]

Though the arch is a large scale monument micro-modeling was chosen here, since it is the only way to properly capture the local behavior around the replaced stone.

## 2.3 FEM method and OOFEM software

### 2.3.1 The Finite Element Method (FEM)

Nowadays, the finite element method is the most spread and the most powerful tool used to solve complex boundary value problems and differential equations. The equations that govern the examined problem are the kinematic equations, the constitutive law of masonry, and the equilibrium equations. Their solution is a function over the domain (displacement, strain, stress). However, the solution might not be analytically found for a complex problem.

Using FEM consists in the discretization of the continuous problem in a finite number of small elements linked together with nodes. On each element, the functions are approximated with suitable functions (the shape functions) and the solutions at nodes are the new unknowns of the problem. The solution is achieved by minimizing the energy (principle of virtual work): this is the passage from the strong form to the weak form, because of the loss of information on the domain.

The refinement of the mesh, the types of elements chosen, and the material properties are important factors and should be considered carefully.

### 2.3.2 OOFEM software

OOFEM is an Object Orientated Finite Element software developed by Bořek Patzák at the Czech Technical University in Prague [20]. It was created as a response for the need of open-source finite element tools in the field of Civil Engineering, where complex problems are faced. OOFEM is an open software using the language C++. It can be adapted to a large range of problems.

It is nowadays an efficient tool that can deal with linear or non-linear static and dynamic analysis. Libraries of elements and of material are provided, and the calculation code can be coupled with 3D mesh generators.

## 2.4 Hypothesis of the model

### 2.4.1 Geometry of the section

The arch is 10 m wide and 0.45 m thick. When unfolded, it measures 25 m long.

Implementing the complete geometry of the arch is a time consuming activity that is not necessary before proposing an efficient model. In Chapters 3 and 4, the difficulties related to the definition of the geometry are explained. In a word, it is only a semi-automatic process. The coordinates of each node must be added manually as well as the position of damaged stones. The units are created row by row, and implementing different heights in the same row is too time consuming at the stage of the creation of the model. It would present an interest only when the model is validate and applied to a specific section to prepare site intervention.

Therefore the section of work is first reduced to a smaller section (see Figure 2.3). This section is considered as relevant because it is big enough to cover several stones: most of the different materials and states of damaged are concentrated in this area. Finally, it is centered enough not to have side effects. However, it also means that in reality the two lateral parts of the bridge around the section will add some support that is not taken into account when studying only the region selected. Studying the reduced area is then a conservative approach. Then, the geometry of the examined section is simplified. The area is  $L_y = 3.5$  m high and  $L_x = 4.5$  m wide. The unit ashlar is 0.7 m high and 0.5 m wide. There are therefore 5 rows of 9 units. In the second model, the stones are bonded with a thin layer of mortar of 0.2 m, and the new geometry is  $L_y = 3.68$  m high and  $L_x = 4.7$  m wide.

The influence of the top infill of the bridge was not taken into account either. Yet, it would add some stiffness and prevent the deformation, so it is conservative not to model it. In a more detailed approach, it would be interesting to find a way to model this increase of stiffness. Yet, it would also require further site studies since for now, no information exists about the properties of the interface between the vertical and horizontal layers of the masonry.

## 2.4.2 Two models

Two models were developed during this thesis in order to overcome the difficulty of the modeling of the reactivation of the newly replaced stone. The two models are described in more detail in the following chapters.

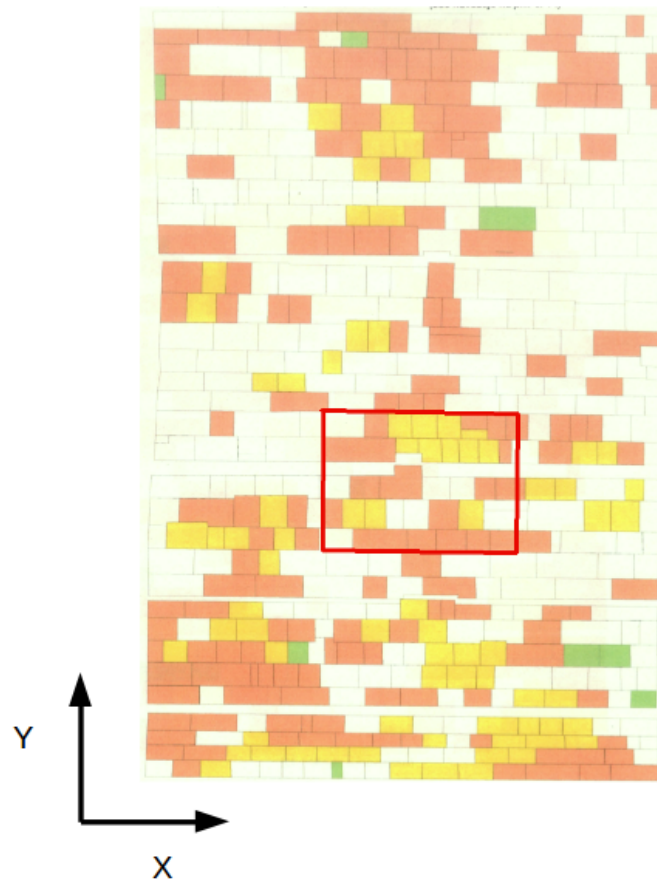
- One model is *homogeneous* and isotropic: only stone units are considered. Though it is really simplified, the good quality masonry and the low thickness of the mortar joint justify this first model. The reactivation of the stone is modeled with eigenstrain boundary conditions.
- The second is *heterogeneous* and is implemented with elements of mortar between stone units. The activation is modeled by applying a uniform distributed load.

## 2.4.3 Type of elements

The arch can be seen as an unfolded element loaded in its plane by the average resultant stress caused by self weight. The problem results in the 2D study of a planar thin structure loaded in only 1 direction, the  $y$  direction (see paragraph 2.4.5). It can thus be assumed that the stresses in the third direction are null ( $\sigma_{zz} = \tau_{xz} = \tau_{yz} = 0$ ). The suitable elements are plane stress elements. In Chapters 3 and 4, the type of plane stress elements used for each model is detailed.

## 2.4.4 Material

In both models, the brick and the masonry are considered individually, with no homogenization of the material. The constitutive laws used for the materials are linear elastic. The use of such simplified constitutive laws underestimates deflections as well as the influenced area by the stone replacement. However, there was a need for efficient modeling hypothesis in order to establish reasonable models to describe the global process. Moreover, as it was explained earlier, this structural analysis does not concern the stability or the ultimate state of the arch. Thus, staying in the elastic domain could be a criterion of the study. It is important to remind this strong hypothesis to understand that the quantitative results about local plastic damage around



**Figure 2.3:** Reduced area of the arch chosen for the study

the replaced stone cannot be considered as accurate, but shall be verified with a refined analysis. The material properties were established according to literature [7]. The values (density, Young's modulus, Poisson's ratio and compressive strength) are summarized in the Table 2.1. One must notice that for the current analysis, only the Young modulus and the Poisson ratio matter.

For a good compatibility of the mechanical properties between the stones in place and the newly inserted one, the Young moduli of the remaining stones and of the new units are taken equal. The weathered stones, on the contrary, have a lower stiffness. Moreover, it would have been interesting for a more accurate model to apply a specific value of Young modulus to each weathered stone according to the material cartography of the arch (see Figure 1.9a), but this



Table 2.1: Mechanical characteristics of the materials

<b>Stone</b>				
	<b>density</b> [kg/m <sup>3</sup> ]	<b>Young Modulus</b> [MPa]	<b>Poisson ratio</b> [.]	<b>compressive strength</b> [MPa]
<b>remaining stone</b>	2023	20200	0,15	9,9
<b>damaged stone</b>	2023	10000	0,15	9,9
<b>new stone</b>	2700	20200	0,15	30,5

<b>Mortar</b>				
	<b>density</b> [kg/m <sup>3</sup> ]	<b>Young Modulus</b> [MPa]	<b>Poisson ratio</b> [.]	<b>compressive strength</b> [MPa]
<b>remaining mortar</b>	1320	2100	0,15	2
<b>damaged mortar</b>	1320	2100	0,15	2
<b>new mortar</b>	1650	2100	0,15	2,5

would require further site investigation about the stones' characteristics.

## 2.4.5 Loading

The loading is adopted according to the thermo-mechanical analysis of the bridge realized in a former study [25]. The effects of all loads, including the self weight, are lumped together and are expressed by a sole stress,  $\sigma_{yy} = 0.5$  MPa, normal to the top section.

In the numerical model, the nodes of the top section are subjected to a master/slave condition, where the top left corner node is defined as the master node. A point force  $F$  is applied at this node. For a section of thickness  $t$  and of length  $L_x$ , the force is:

$$F_{top} = \sigma \times S = \sigma \times t \times L_x = 0.5 \times 0.45 \times L_x \quad [\text{MN}]$$

## 2.4.6 Boundary conditions

The boundary conditions are summarized in Figure 2.4.

**Top edge** The vertical degree of freedom of the nodes on the top edge is subjected to the master/slave condition described earlier. All the nodes therefore have the same vertical displacement.

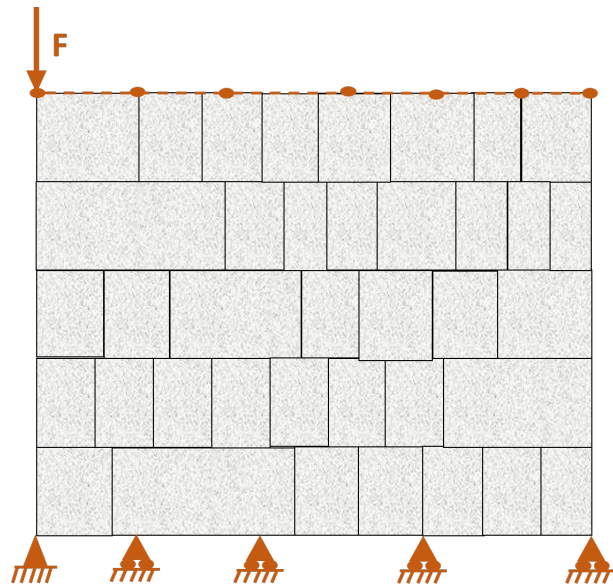


Figure 2.4: Boundary conditions applied to the section

**Bottom edge** The arch is simply supported on its bottom edge. The left bottom node is constrained in both  $x$  and  $y$  directions. The other nodes are constrained in the  $y$  direction.

**Lateral edges** At the scale of the whole arch, the side are free of constraint. When studying a reduced area of the arch, in a more accurate model, it could be interesting to add some truss elements in order to model the presence of the lateral pieces of good stones that redistribute the compressive stress, especially when the replaced stone is on the extreme sides of the smaller section.

## 2.5 Presentation of the results

Many information can be taken out the FE analysis and are of interest to describe exhaustively one specific case of replacement. In the following chapters, only specific values are studied to fulfill the objective of building a suitable computational model.

### Deformation

As explained earlier, the chosen procedure of replacement of the stones should minimize the vertical deformation. To calculate it, the vertical displacement of the top left node of the model is recorded. Deformations are then calculated as follows:

$$\varepsilon_{global} = \frac{|w_{\text{top left node}}|}{L_y}$$

where  $L_y = 3.68$  m is the height of the section of arch studied and  $H = 0.7$  m is the height of the stone.

Since the model is simply supported, it is also important to examine the horizontal displacement  $u$ .

### Increase in stress concentration

In the following chapters, the stress distribution more often refers to the compressive stress in  $y$  direction:  $\sigma_{yy}$  (negative values for compression). The stress in the other direction,  $\sigma_{xx}$ , and the shear stress  $\tau_{xy}$  are other relevant quantities.



# Chapter 3

## Homogeneous model

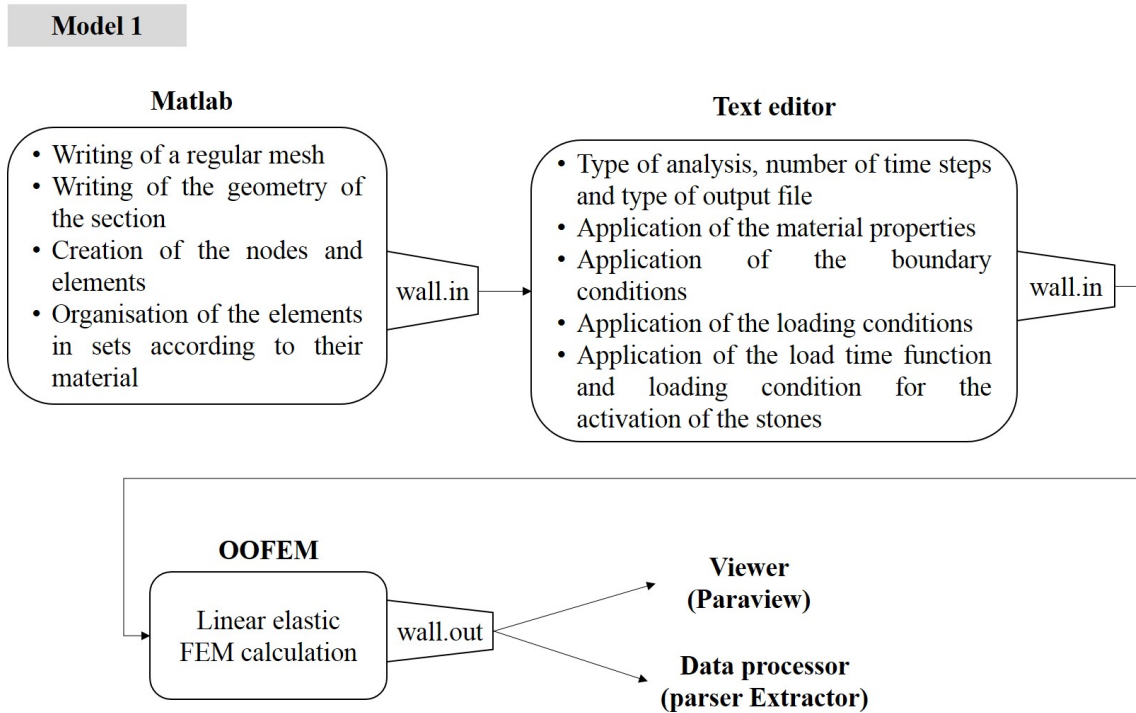
### 3.1 Description

#### 3.1.1 General idea

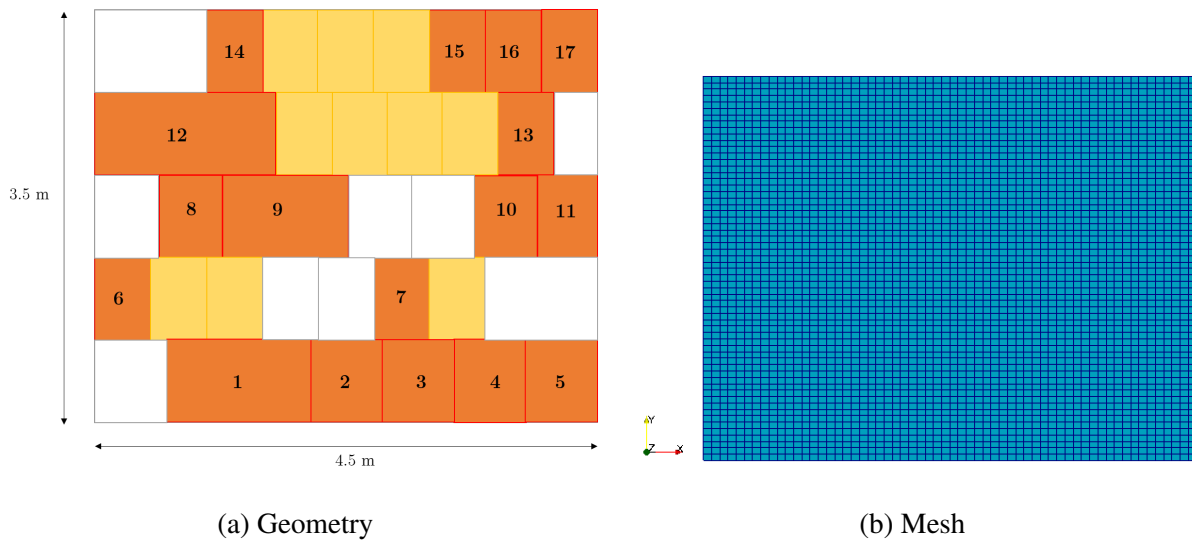
This model only considers ashlar units of sandstone, with no mortar: it is homogeneous and isotropic. The stones are arranged side-by-side with no interface between two units, the mechanical properties only depend on the state of damage of each stone. The linear constitutive law of the material and the homogeneity of the model make it a very simplified approach. That way, it is possible to roughly model the behavior of the section of arch when a stone is replaced. Since the material is linear elastic, the solution is obtained without iterations in a very reasonable computational time. One can notice that compared to the size of the stone blocks, the layers of mortar are very thin (0.02 m), therefore it makes sense to assume that the response of a model composed of stones only can be treated as representative of the real behavior.

#### 3.1.2 Creating the computational model

First, a script in Matlab [16] is used to generate a regular finite element mesh with  $60 \times 60$  elements, then the geometry of the section is drawn to match the mesh (see Figure 3.2). After that, the construction stages, and the stones and the corresponding finite elements to be removed and inserted are defined. Finally, the loading and boundary conditions are listed in the input file.



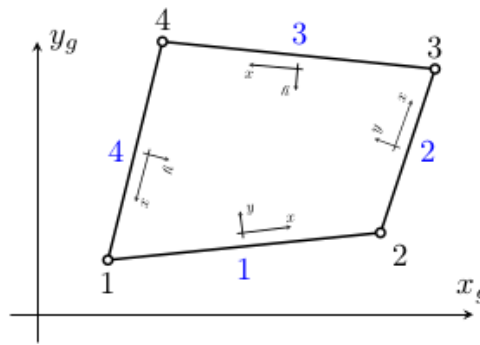
**Figure 3.1:** Flowchart of the homogeneous model



**Figure 3.2:** Geometry and mesh of the reduced area implemented in the homogeneous model

The building process of the final file is summarized in Figure 3.1.

The elements that are used are isoparametric quadrilateral, 4 nodes, plane-stress elements.



**Figure 3.3:** Plane stress element used for the homogeneous model

Each node has 2 degree of freedom ( $x$  and  $y$ ), and there are 4 Gauss integration points for the element (see PlaneStress2d in OOFEM, Figure 3.3).

### 3.1.3 Modeling the new stone activation

#### 3.1.3.1 Timeline of the process

At the beginning of the replacement process, the elements that constitute the damaged stone block disappear. New elements constituting the new stone appear, and they are submitted to eigenstrain that increases in time until reaching a satisfactory stress distribution in the newly inserted stone. The activation using eigenstrain is detailed in the following paragraphs. To one stone unit that requires restoration, correspond two sets of elements that have exactly the same coordinates. The first set is called *old stone*, the second *new stone*. Load time functions are applied to the two sets:

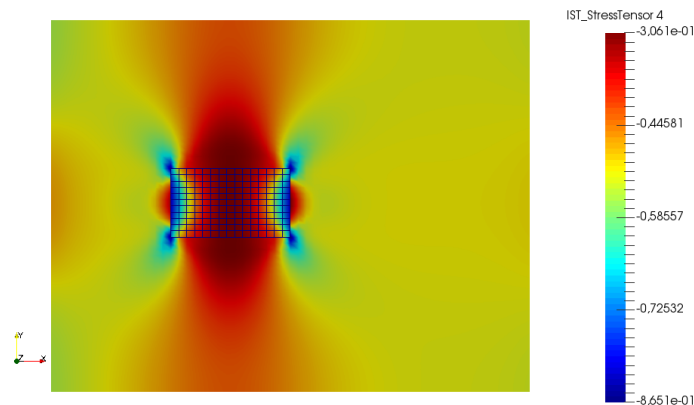
- *new stone*: at the beginning the elements are present and have the stiffness of damaged stones. At the time step corresponding to the removal, the elements disappear.
- *old stone*: until the time step corresponding to the removal, these elements are present with almost null stiffness. After the removal, the stiffness value increases to the stiffness chosen for new pieces of stone (see Figure 2.1). Then loading is applied to the elements as described in next paragraph.

Using this eigenstrain procedure, it is not necessary to constrain the unsupported degrees of

freedom once the old stone has disappeared.

### 3.1.3.2 First attempt: uniform eigenstrain loading

In this attempt, uniform eigenstrain is applied to the stone unit. Eigenstrain is usually introduced to capture stress-independent effects, such as thermal expansion and shrinkage. In such cases the eigenstrain is for most of the materials isotropic [10]. Here the eigenstrain is used to generate a compressive stress simulating the process of activation in a newly inserted stone unit. Compared to the previously mentioned fields of application, the current eigenstrain has only one non-zero component corresponding to the vertical direction, the direction of the stress activation.



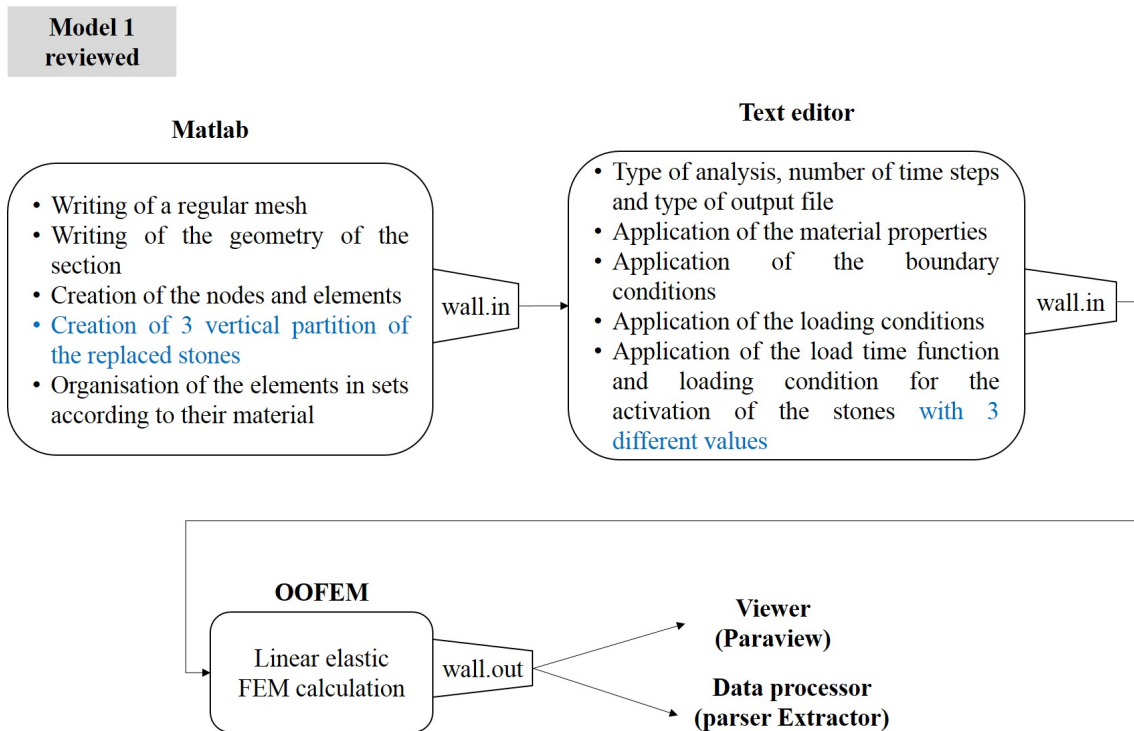
**Figure 3.4:** Distribution of  $\sigma_{yy}$  [MPa] caused by uniform eigenstrain loading of the inserted stone

In order to get rid of the side effects at the edges of the model, the first attempt is made on the central stone 9. However, the resulting stress distribution is not uniform. The Figure 3.4 reveals that the stress distributes in the stone in the shape of a cone. It is very close to what can be observed in a compression test, with reversed values (here, the core is less loaded than the edges). The values between the core and the edges vary in a range of 0.55 MPa, which is as high as the external loading. At the moment when the stone is removed, the internal stress is redistributed and concentrates on both lateral edges of the hole. When activating the new unit, the stress is still concentrated on the edges, though the stone was supposed to be reloaded uniformly. On site however, the distribution of the stress when reactivating the stone should be opposite: the wooden wedges are closer to the middle of the stone and the stress tends to be



higher in the middle than on the edges.

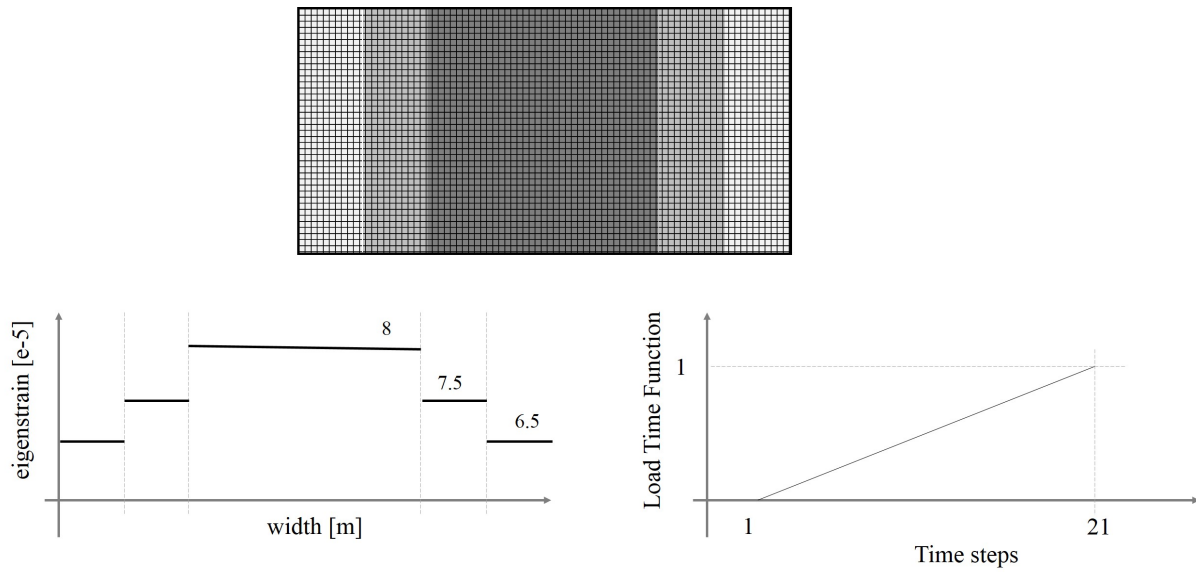
### 3.1.3.3 Second attempt: piecewise constant eigenstrain loading



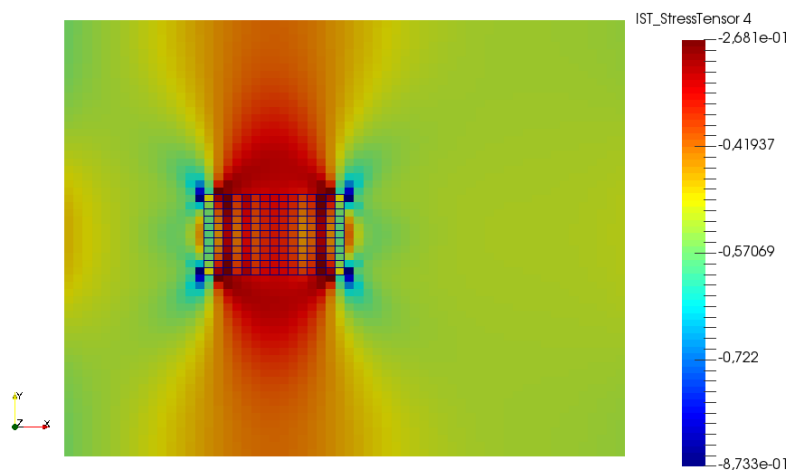
**Figure 3.5:** Revised flowchart of the homogeneous model

From the previous result, it seems that achieving a perfectly uniform stress distribution in the newly inserted stone after its reactivation presents a difficulty. In a second attempt, the stone is loaded with piecewise constant eigenstrain, so that the extreme edges are less loaded than the inner core. The new piece of stone is divided into 6 vertical sections, and each section is loaded with a specific value, element by element, symmetrically to the vertical middle axis (see Figure 3.6). The new chart of the model is presented in Figure 3.5. However, in Figure 3.7, it can be observed that the final stress is still not uniform.

This non uniform loading solution is not satisfying either. Step by step, suitable values could be found to achieve a uniform distribution of stress. Yet, loading values are dependent on the width and on the stiffness of the stone, which means that a specific function should be established by hand for each replaced stone. Finally, it would be time consuming to prepare



**Figure 3.6:** Non uniform distribution of eigenstrain to activate the new stone, applied to vertical sections multiple of  $1/6$  of the stone width



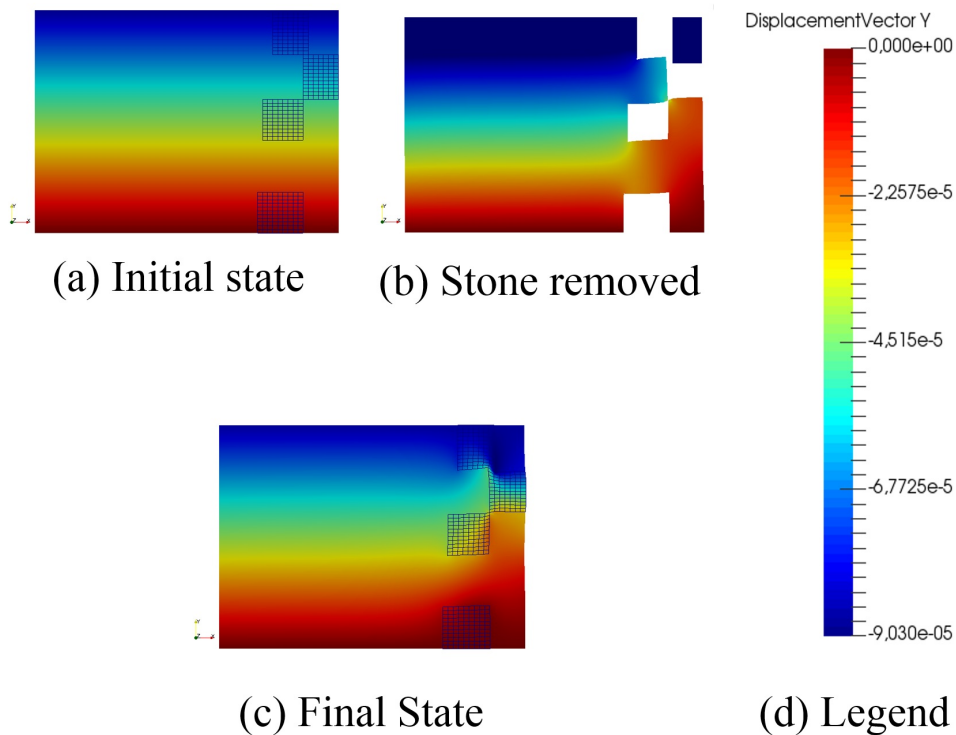
**Figure 3.7:** Distribution of  $\sigma_{yy}$  [MPa] caused by piecewise eigenstrain loading of the inserted stone

the model. Moreover, dividing the stone into 6 vertical sections is more and more complex for a narrower stone and there is a risk that some elements are forgotten when sorted out automatically. All those constraints make this modeling approach a laborious job that is hardly applicable to the entire arch.

## 3.2 Model of the reduced area of the arch

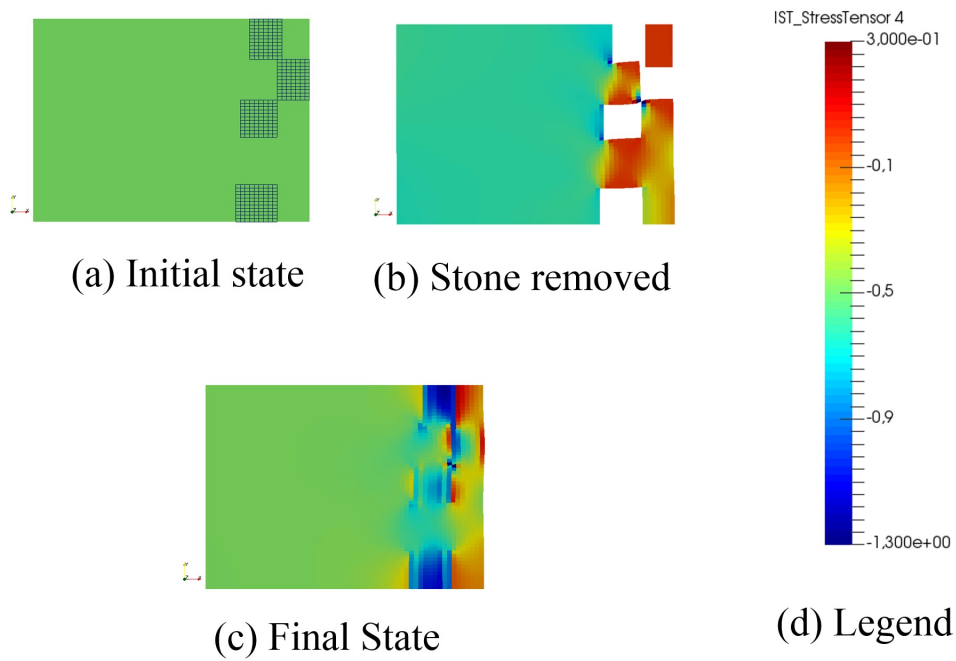
In this section, the whole area of study is modeled. 3 cases are studied: the removal of one column, the removal of one row, and finally the removal of 4 columns in 4 stages.

### 3.2.1 Replacement of one column

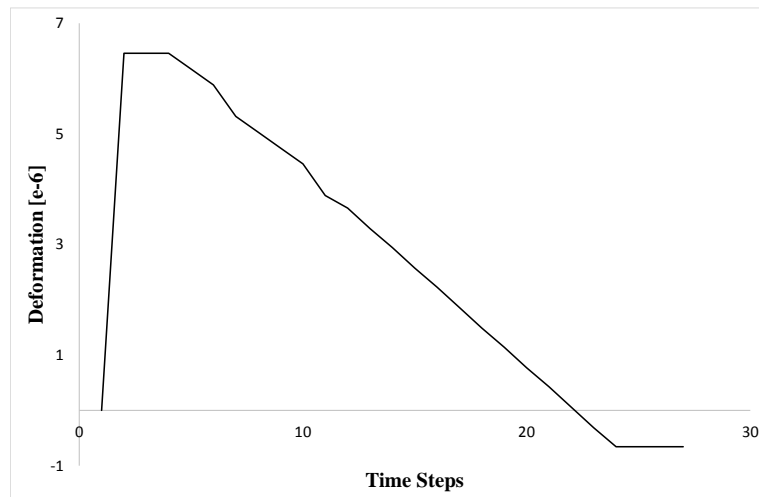


**Figure 3.8:** Vertical displacement [m] in the homogeneous model when restoring 1 column (deformed shape  $\times 2000$ )

First, a whole column is removed (stones 16, 13, 10, 4). The resulting stress  $\sigma_{yy}$  and the vertical displacement and deformation are presented in Figures 3.10, 3.8 and 3.9.

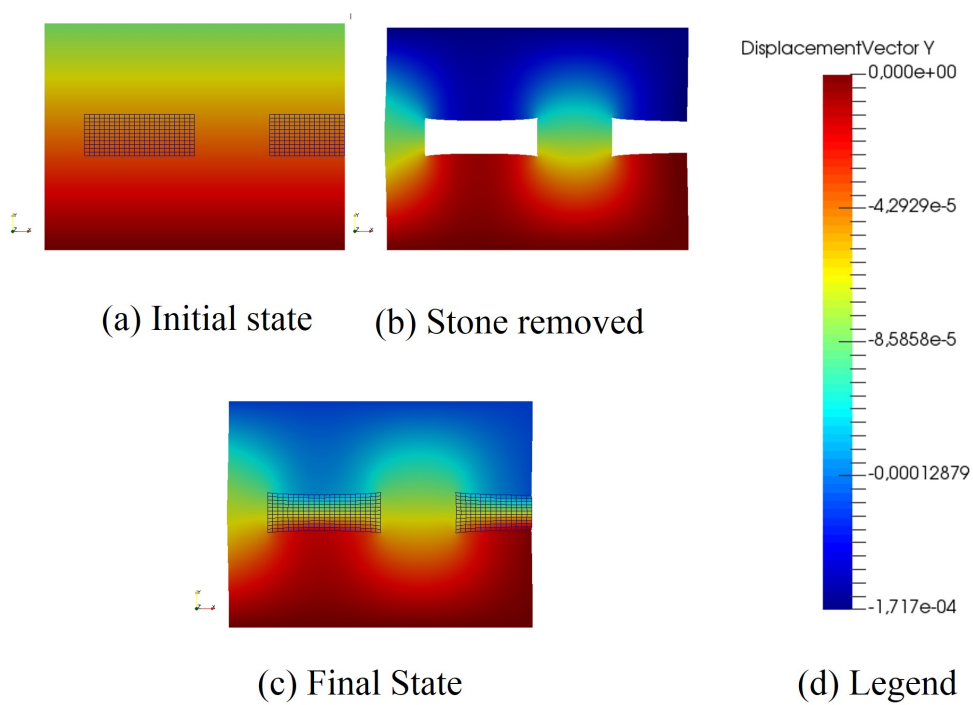


**Figure 3.9:** Distribution of  $\sigma_{yy}$  [MPa] in the homogeneous model when restoring 1 column (deformed shape  $\times 2000$ )



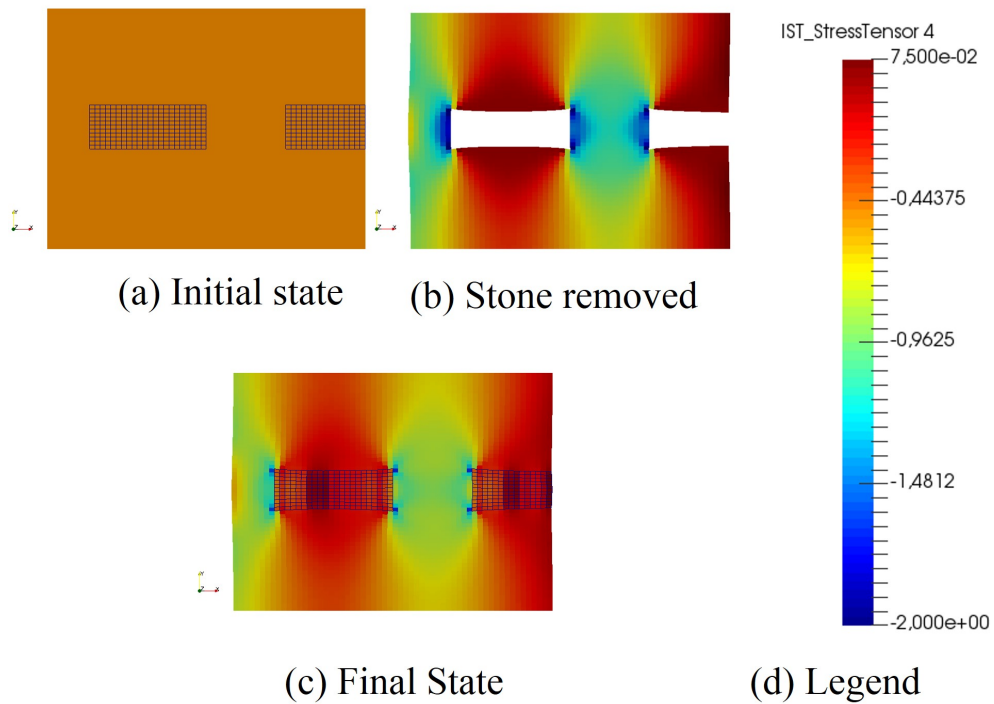
**Figure 3.10:** Vertical deformation [m] in the homogeneous model in time when restoring 1 column

### 3.2.2 Replacement of one row

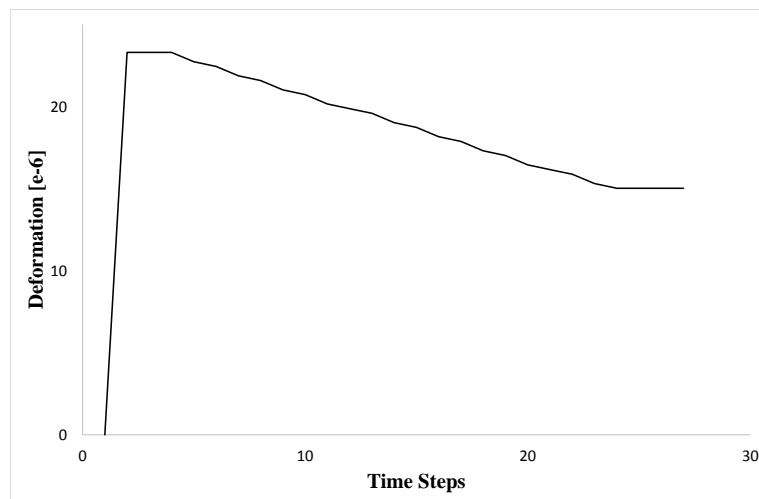


**Figure 3.11:** Vertical displacement [m] in the homogeneous model when restoring 1 row (deformed shape  $\times 2000$ )

In this section, a whole row is removed (stones 8, 9, 10, 11). The resulting stress  $\sigma_{yy}$  and the vertical displacement and deformation are presented in Figures 3.11, 3.12 and 3.13.



**Figure 3.12:** Distribution of  $\sigma_{yy}$  [MPa] in the homogeneous model when restoring 1 row (deformed shape  $\times 2000$ )

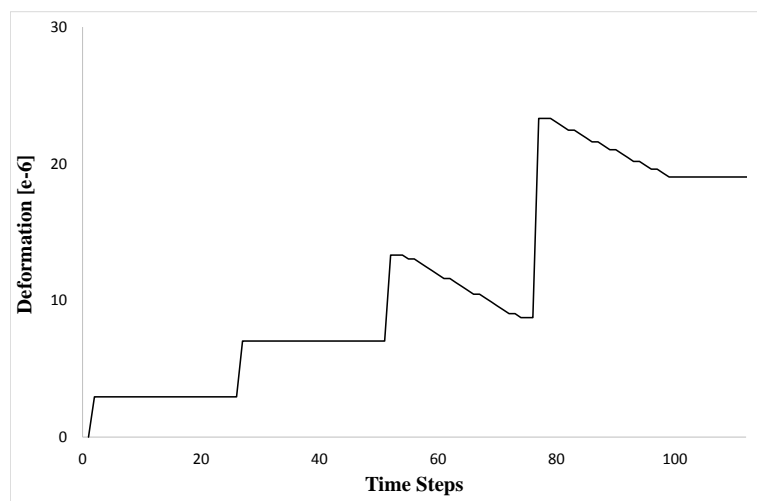


**Figure 3.13:** Vertical deformation [m] in the homogeneous model in time when restoring 1 row

### 3.2.3 Replacement of 4 columns

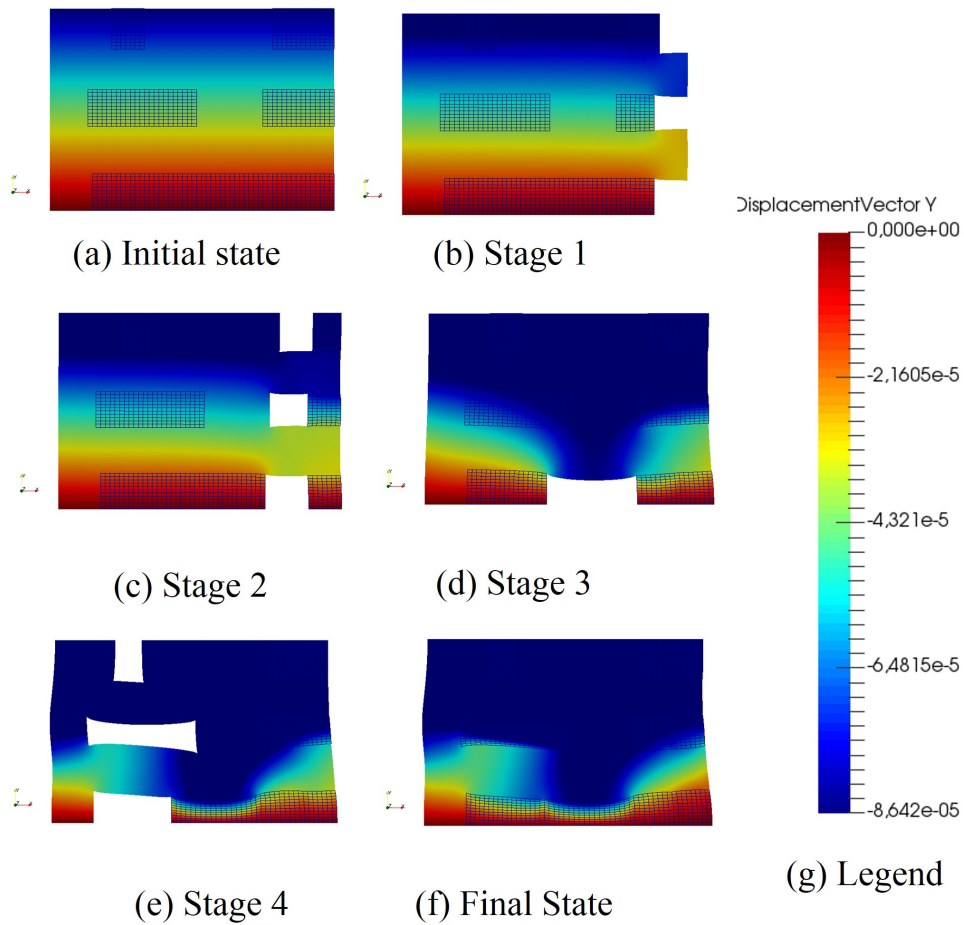
Finally, the modeling strategy is applied to remove almost all the damaged stones of Figure 3.2a. It was decided to remove the stones column by column according to the conclusions presented in Section 3.2.1. The area to restore is divided into 4 columns, each column is restored in one stage. However, it was noticed that the local deformation around removed stones is too high to be consistent when 2 stones, one on top of the other, are replaced. This is linked to the poor capability of the model to capture the reactivation procedure. Therefore, only 3 rows out of 5 are restored in the first approach. The combination is:

- stage 1: stones 17, 11, 5
- stage 2: stones 16, 10, 4
- stage 3: stones 2, 3
- stage 4: stones 14, 9, 8, 1



**Figure 3.14:** Vertical deformation [m] in the homogeneous model in time when restoring the reduced area column by column in 4 stages

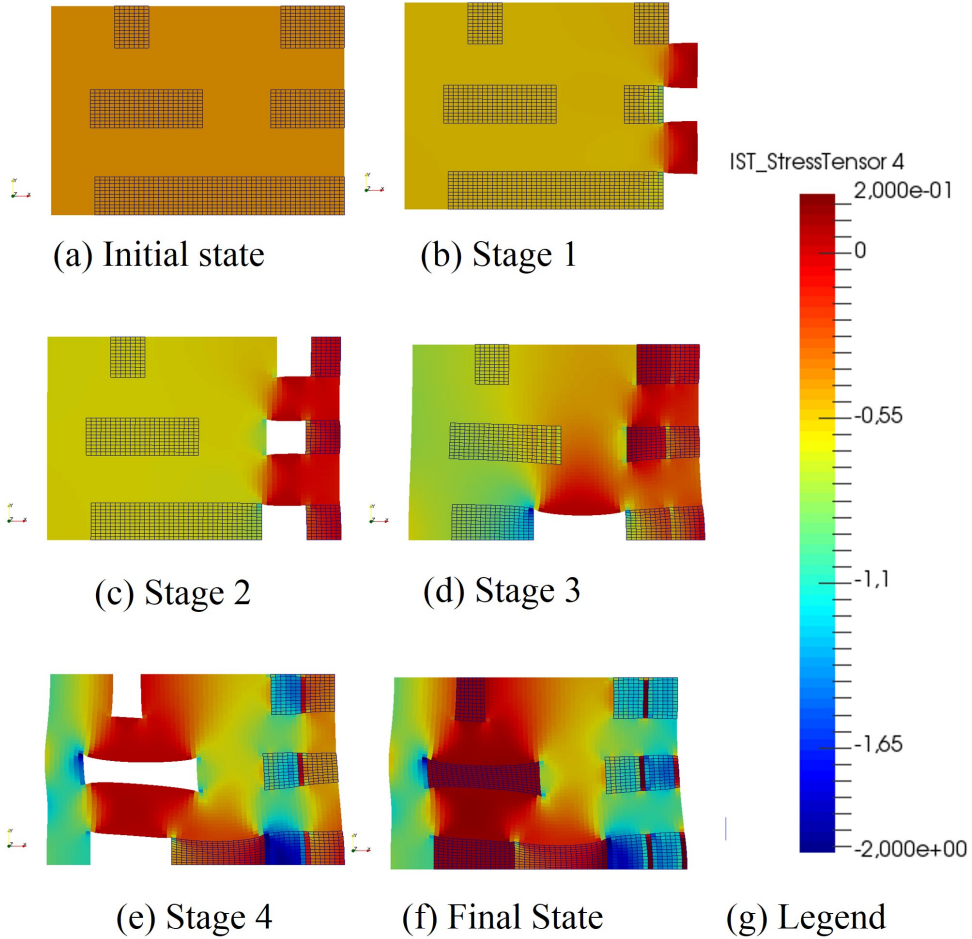
The Figures 4.26 and 3.14 are consistent with the conclusion of the paragraph 3.13. The global deformation is linked to the width of the column that is restored. The Figure 4.27 fosters



**Figure 3.15:** Vertical displacement [m] in the homogeneous model when restoring 4 columns (deformed shape  $\times 3000$ )

the importance to develop a refined model to describe the increase of stress around the replaced stone. Indeed, tensile stress seems to appear at the corner of the stones. Though these values are not accurate, attention should be paid to those particular areas.





**Figure 3.16:** Distribution of  $\sigma_{yy}$  [MPa] in the homogeneous model when restoring 4 columns (deformed shape  $\times 3000$ )

## 3.3 Discussion on the model

### 3.3.1 Capabilities of the model

It is from the global point of view that this model can be helpful. Though the reactivation procedure cannot be captured, the global behavior is still relevant without it. Indeed, because of the homogeneity of the material and the simplicity of the geometry, it can run quite fast. Using this approach, many different combinations of replacement procedures could be analyzed without bothering for the reactivation, and trying only to minimize the global deformation.

Further studies could be carried out with this model to understand the influence of certain parameters on the global deformation:

- the maximum width of a column of stones that can be removed during one stage, compared to the width of the restored area
- the maximum area of stone that can be replaced during one stage
- the minimum number of stages that are needed to replace all the stones

### 3.3.2 Limits of the model

This homogeneous isotropic model cannot be used to describe the reactivation of a new stone unit during the process of replacement of elements of historical masonry. Since it cannot capture correctly the response during activation it does not make sense to analyze the local stresses around the replaced stone, though it is important to check that there is no local damage due to tensile stress for instance.

From a computational point of view, preparing a model is complex. The geometry of the stones must match the mesh, though it is irregular - most of the time, the geometry is first drawn, then the mesh is applied to it. Moreover, the geometry is built up by creating the stones row by row, which is a limit for the cases when the stones do not have the same height on one row. This was not a problem for the Charles Bridge, since the masonry is quite regular. The topology of the replaced stone must also be specified manually, which starts to be a problem

when the number of stones increases. In Figure 3.8, it can be noticed that the top right stone that stays in place during the replacement process does not have proper boundary conditions for the combination chosen. For each new combination, specific complexities appear either linked to the boundary conditions of the surrounding stones. This study shows another limit of this semi-automatic model. Therefore general recommendations should be found from quite simple combinations before building one complex and exhaustive model.

In conclusion, this model is not suitable for big, irregular structures where the inserted components need to be activated.



# Chapter 4

## Heterogeneous model

### 4.1 Description

This model is heterogeneous and takes into account the presence of 0.02 m mortar layers. In order to describe the activation procedure, the former homogeneous model used eigenstrain conditions on the newly inserted stone. In this model, the loading of the new stone unit is modeled with a stress applied in the vertical direction on the newly inserted stone.

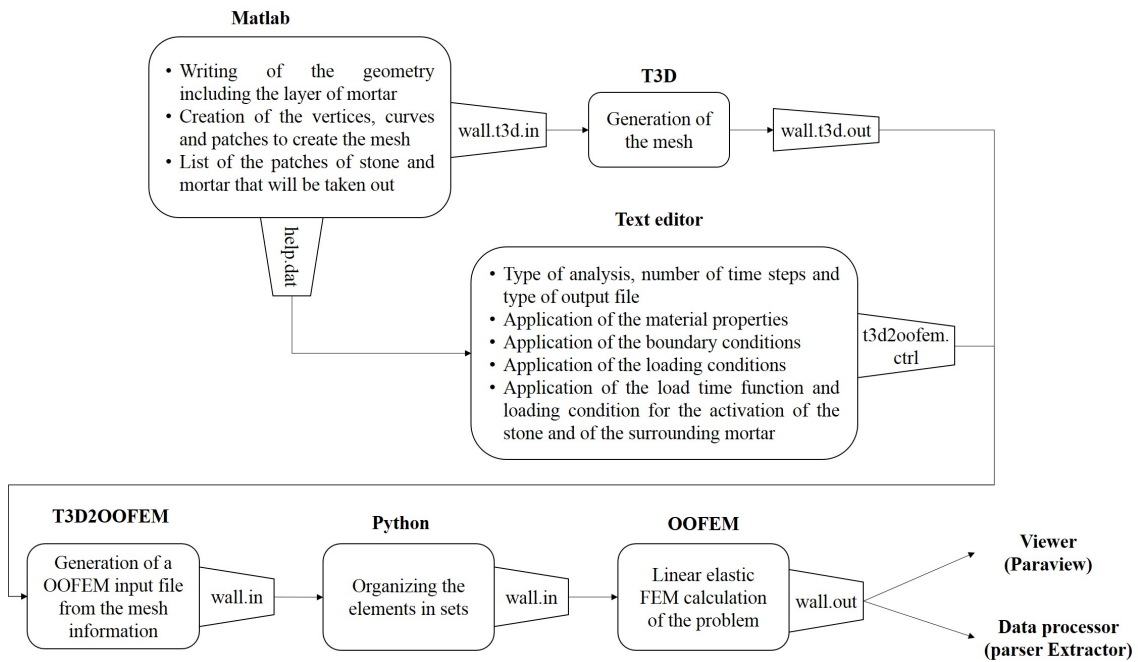
#### 4.1.1 Creating the computational model

Several softwares are used to build this model. First the geometry is written in Matlab, then the mesh is generated automatically with T3D [24]. From this mesh, an input file for OOFEM is built. The different steps are summarized in the Figure 4.1.

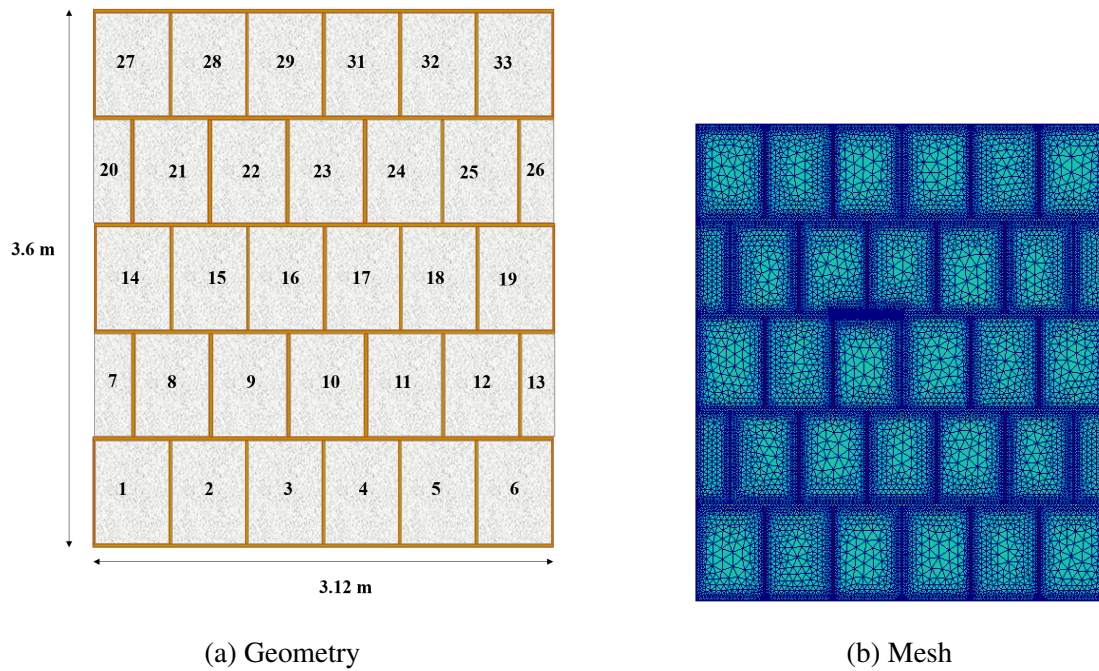
The heterogeneous model is made of perfectly regular coursed masonry in order to minimize the number of parameters of the model and to focus on the modeling of the reactivation phenomena (see Figure 4.2a). The stones will be referred as they are numbered in this scheme. For this model, the stones coordinates are generated automatically with Matlab and are stored in an array, so that the sets of replaced stone can be changed easily.

For the meshing, the stones and the mortar layers are defined in patches, each patch is then meshed automatically according to the size of element required. This means that each unit of stone is a single patch, surrounded with at least 8 rectangular mortar patches (3 at the top and

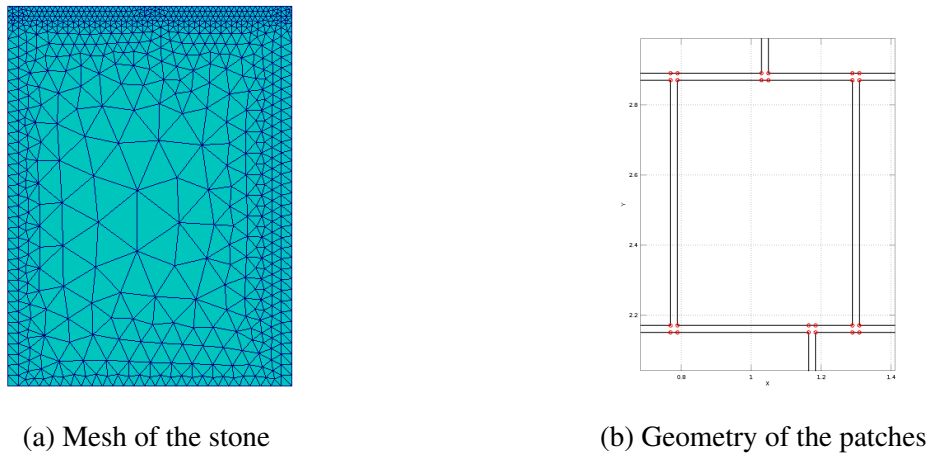
**Model 2**



**Figure 4.1:** Flowchart of the heterogeneous model



**Figure 4.2:** Geometry and mesh of the reduced area implemented in the heterogeneous model

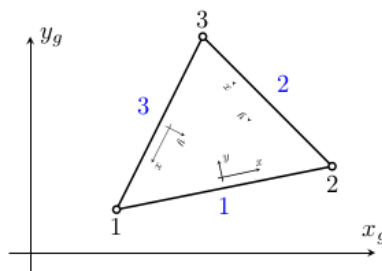


(a) Mesh of the stone

(b) Geometry of the patches

**Figure 4.3:** Zoom of the modeling of one stone and surrounding mortar of the heterogeneous model

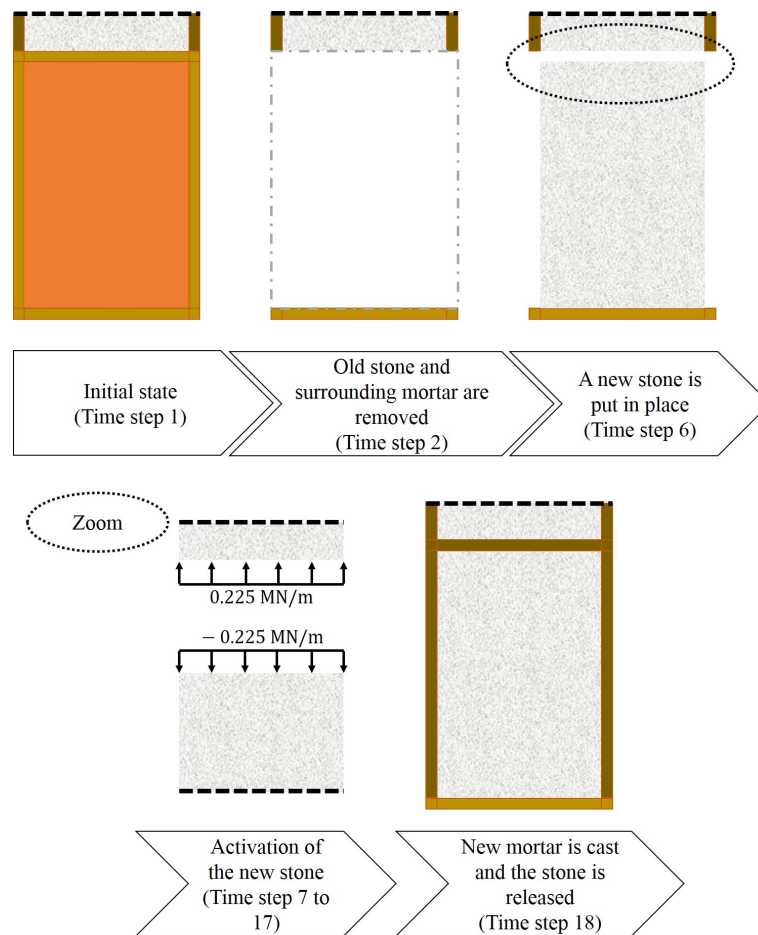
bottom, and 2 on the sides, as in Figure 4.3b). In the Figures 4.2b and 4.3a, the mesh can be observed. The stone is meshed with rough elements, meanwhile the mortar patches are refined. The top patches, especially, present numerous elements. As explained in paragraph 4.1.2, it is required for the boundary conditions of the stone during the reactivation. In total, the model counts 15491 nodes and 30569 elements (this number varies with the number and size of stones to be restored. Here it corresponds to the replacement of one regular unit). The elements that are used are triangular, 3 nodes, with a constant strain plane-stress elements. Each node has 2 degrees of freedom, and there is 1 Gauss point for the element (see TrPlaneStress2d in OOFEM, Figure 4.4).



**Figure 4.4:** Plane stress element used for the heterogeneous

### 4.1.2 Modeling the new stone activation

The first study focuses on the replacement of one stone, the stone 16, that is in the middle of the model to avoid side effects (see Figure 4.2a). It enables to understand the consequences of the replacement process for one single stone. The procedure of replacement is described here in detail and is always the same (see Figure 4.5). Similarly to the homogeneous model, to one weathered stone correspond two sets of elements: one with poor properties (damaged stone) and another one with good properties (new stone).



**Figure 4.5:** Process of activation of the new stone for the heterogeneous model



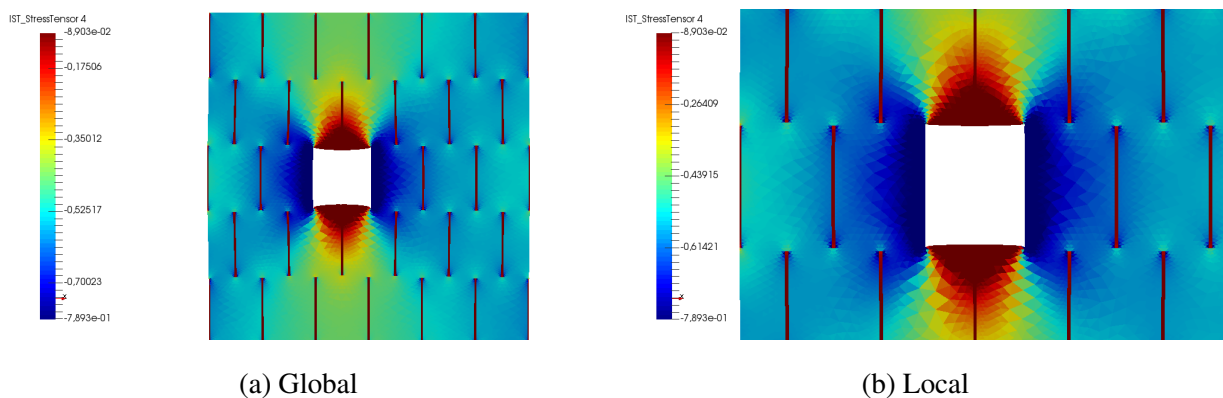
### 4.1.2.1 Process of replacement

**Time step 1** First, the model is vertically loaded by constant line load. The stress is uniformly equal to  $-0.5$  MPa if the material properties are uniform. In the case when the mortar has a lower stiffness, the stress distribution is equal to  $0.519$  MPa in the stones.

#### Time step 2

The damaged stone elements vanish. In OOFEM, the presence of the damaged stone elements is submitted to an activity time function equal to zero after time step 1.999. If this function is equal to zero, the corresponding elements are not considered in the analysis.

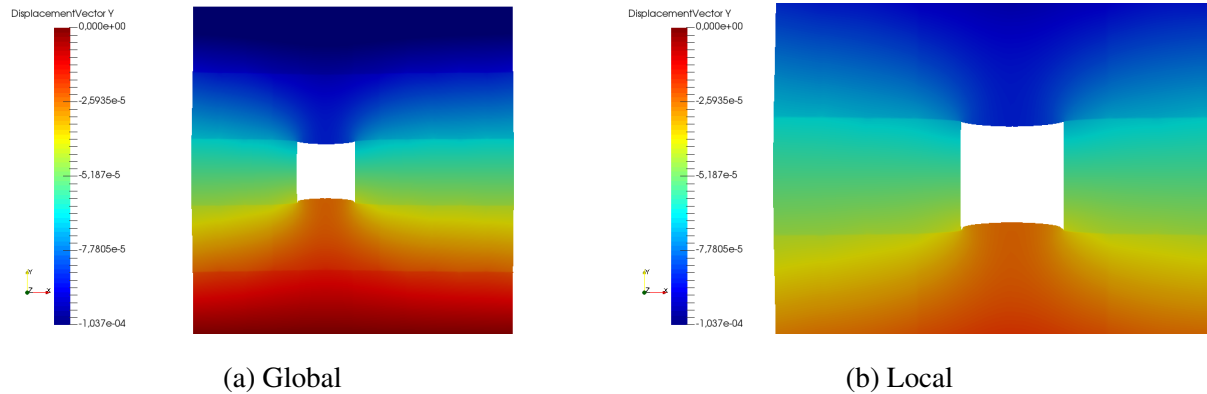
In Figure 4.6, one can observe that the stress is concentrated around the hole, with an increase of stress close to 60 % of the initial value. These values are not accurate, but it gives a first idea of the new stress distribution when a stone is removed. There is also a peak of deformation, both globally and around the hole (see Figure 4.7).



**Figure 4.6:**  $\sigma_{yy}$  distribution [MPa] in the heterogeneous model when restoring 1 stone

#### Time step 6 to 17

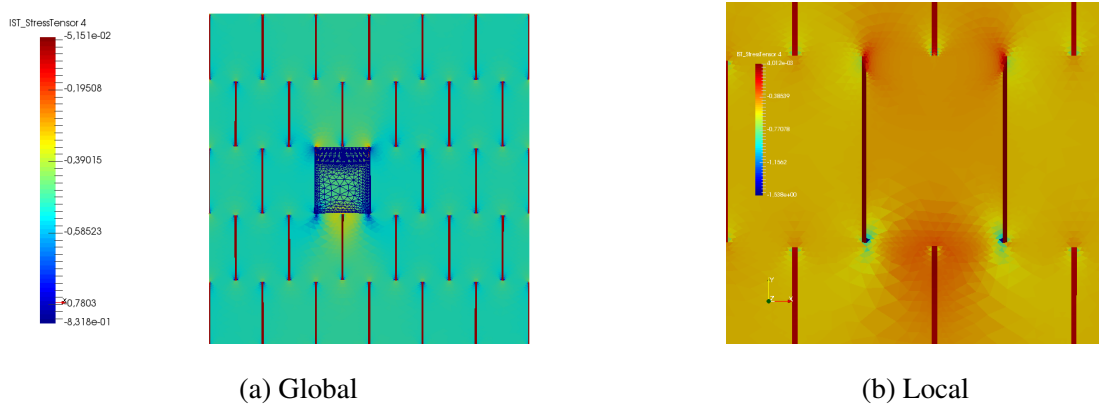
At time step 6, the set of elements of the new stone is cast. From the time step 6 to 17, the stone is linearly reactivated with a uniform distributed load on the top of the new stone and on the opposite bottom of the above stone. For this reason, the top patches of mortar needed to be more refined than the others, so that all patches could be properly loaded (see Figure 4.3b). The activation is completed when the distributed line load reaches  $0.5$  MPa.



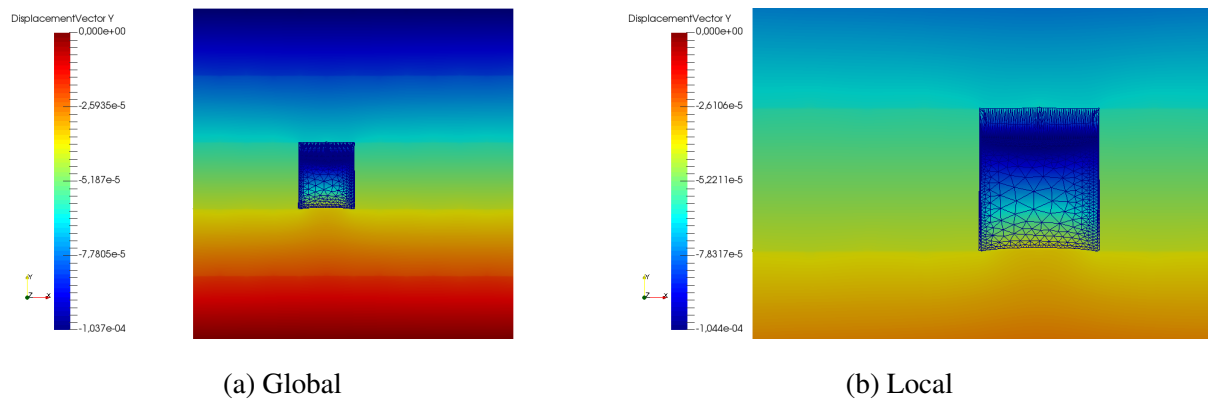
**Figure 4.7:** Vertical displacement [m] in the heterogeneous model when restoring 1 stone (deformed shape scale  $\times 1000$ )

### Time step 18

At time step 18, the new mortar is cast and the stone pressure is released: the time function that increased between step time 6 and 17 falls to 0. The final state of stress is presented in Figure 4.8. The deformed shape is in Figure 4.9, and it is also interesting to see the final values in Figure 4.13. The final stress is not exactly uniform, it is almost 8 % higher in the new stone (see figure 4.14). This is due to the fact that during the activation, the stone is still linked to the structure with the layer of mortar at the bottom. The interface between stone and mortar is perfect, so the Poisson effect leads to a stress concentration under the stone (see the reddish aureole). This is close to what would happen on site since there is friction between the new stone and the wooden wedges which support it.



**Figure 4.8:** Final  $\sigma_{yy}$  distribution [MPa] in the heterogeneous model when removing one stone



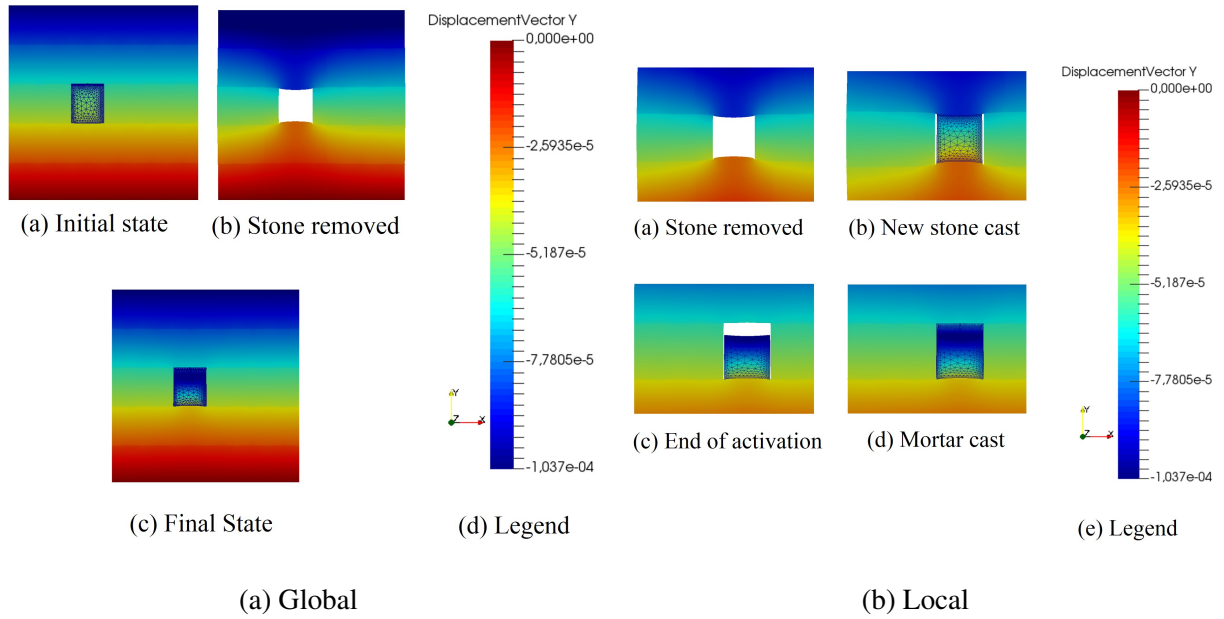
**Figure 4.9:** Final vertical displacement [m] in the heterogeneous model when restoring 1 stone (deformed shape scale  $\times 1000$ )

#### 4.1.2.2 Visualization of the procedure

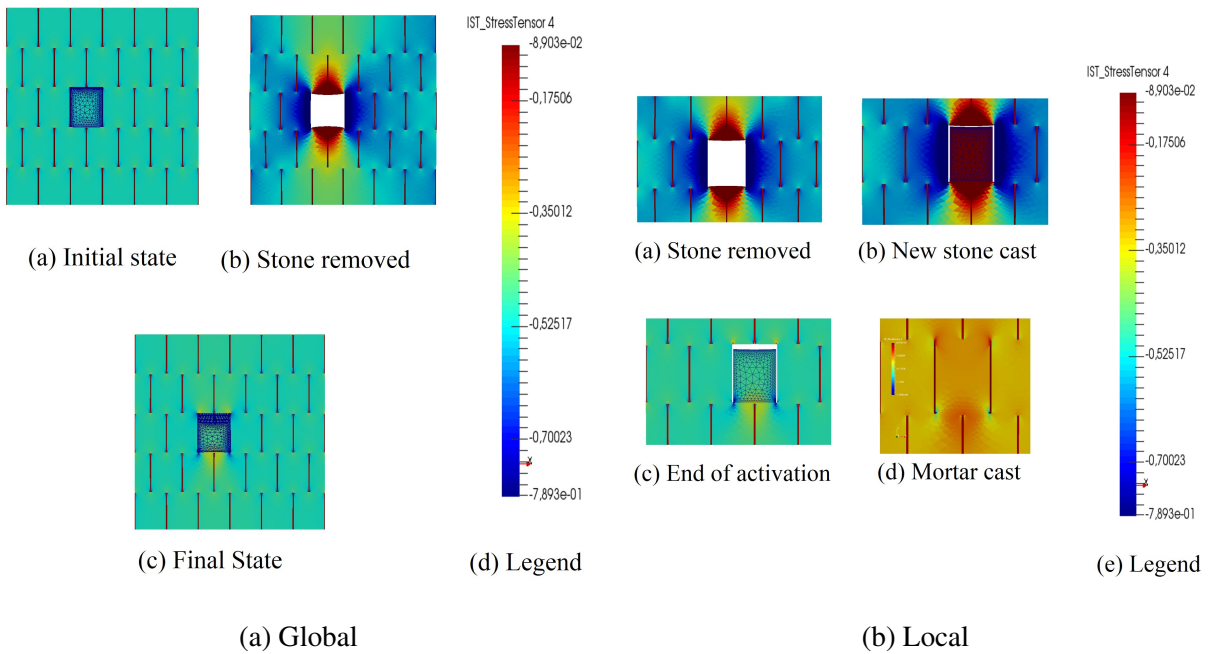
The following figures (Figures 4.10, 4.11 and 4.12) present the vertical displacement, the normal stress  $\sigma_{yy}$  and the shear stress  $\tau_{xy}$  in the model at the different important stages.

#### 4.1.2.3 Deformation of the examined reduced area

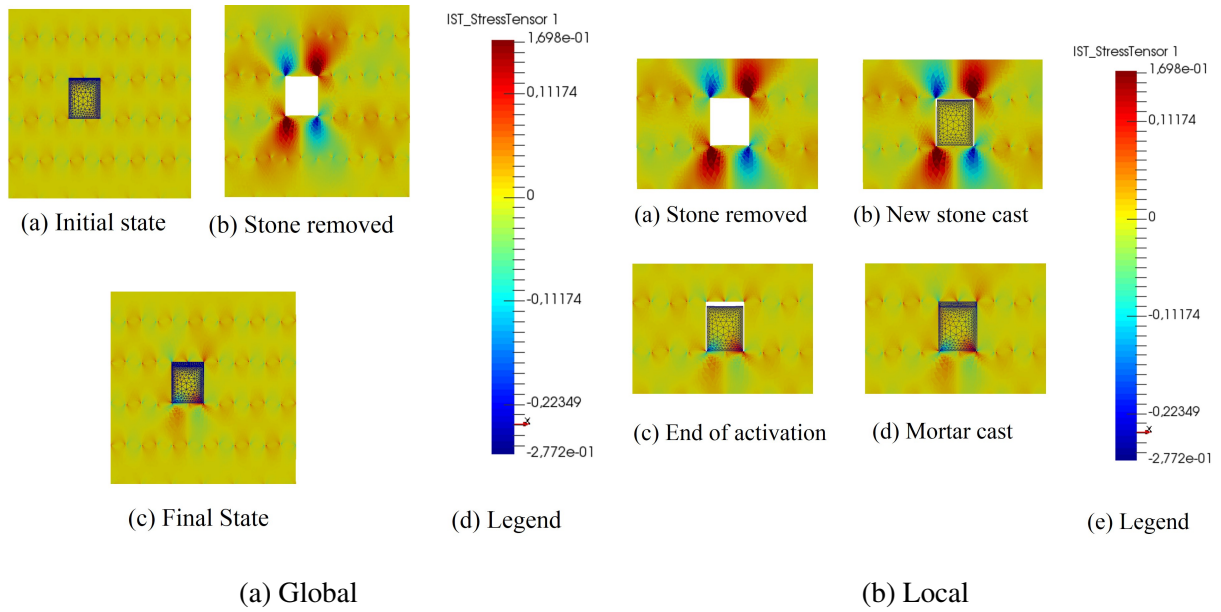
The following graphs present the deformation of the whole model and in the restored stone in time. A peak can be observed when the stone is removed.



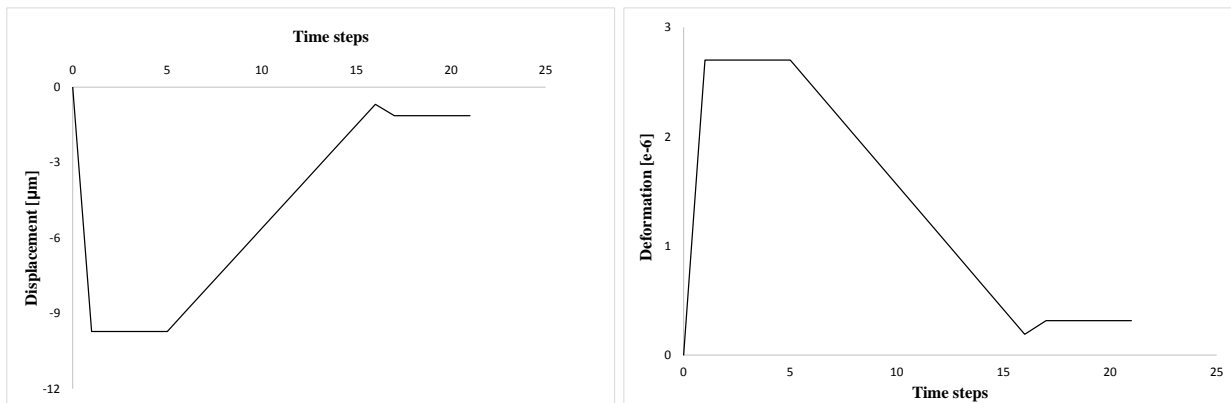
**Figure 4.10:** Vertical displacement [m] in the heterogeneous model for different time steps (deformed shape scale  $\times 2000$ )



**Figure 4.11:**  $\sigma_{yy}$  distribution [MPa] in the heterogeneous model for different time steps (deformed shape scale  $\times 3000$ )



**Figure 4.12:** Shear stress  $\tau_{xy}$  [MPa] in the heterogeneous model for different time steps (deformed shape scale  $\times 2000$ )

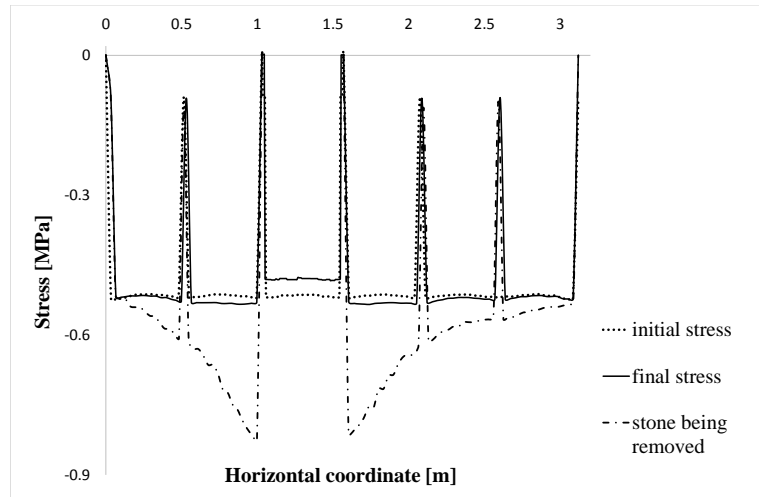


(a) Vertical displacement in time of the top left node of the heterogeneous model (b) Vertical deformation in time of the heterogeneous model

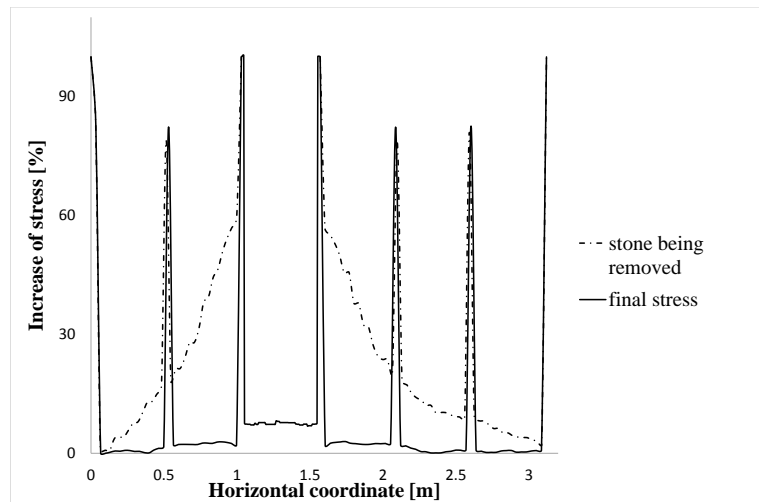
**Figure 4.13:** Behavior of the heterogeneous model during the replacement process

#### 4.1.2.4 Stress distribution in the section

It is interesting to see the stress distribution in the section along the horizontal axis passing through the middle of the removed stone. The stress is captured at different stages of the



(a) State of stress



(b) Comparison to the initial state of stress

**Figure 4.14:**  $\sigma_{yy}$  stress distribution in the heterogeneous model for different time steps

replacement. Then the increase of stress compared to the initial state is calculated. The peaks correspond to the mortar location and are of no interest except to understand the topology of the examined section. One can observe that there is a stress concentration around the stone when it vanishes. However, the final area of influence of the stone is limited in space since the stress goes back to its initial value 0.5 m away from the restored stone.

#### 4.1.2.5 Difficulties of modeling

This heterogeneous model is more satisfactory to capture the phenomenon of the reactivation procedure.

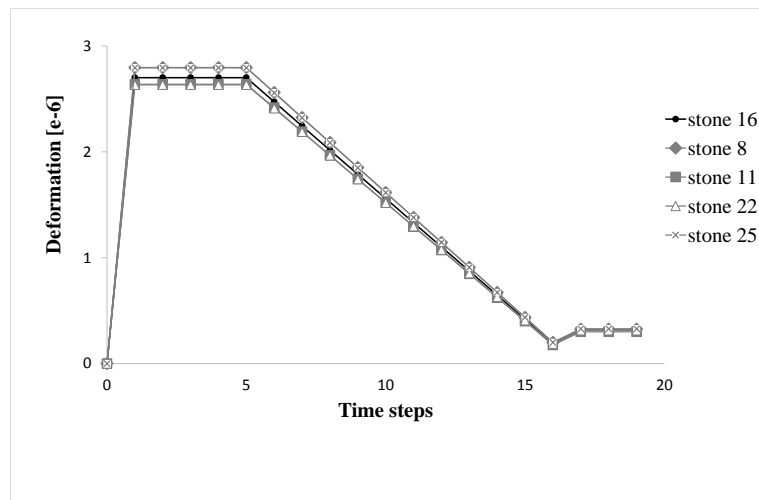
The first difficulty was to treat the case when two adjacent stones must be restored, either during the same stage or in consecutive stages. These stones share the same patches of mortar (see Figure 4.3b), so the patches of mortar experience different histories of loading.

This leads to the second difficulty linked to the construction of the model. The apparition and disappearance of elements are ruled by time functions. Unique time function must be applied to the elements of mortar that are shared between several stones, and the function depend on the stages of replacement of both adjacent stones. In the present study, a model was developed to cover 4 stages. Implementing a new stage is more and more laborious and the risks to forget elements in the application of loads and time function get more and more important. Therefore, if this modeling strategy is used for bigger structure, it is necessary to develop a numerical code that can handle automatic application of the time functions.

Finally, this way of reloading the stone by applying a stress on the top stone and on the replaced stone makes it impossible to replace two stones on top of each other in the same stage for now. In a refined model, boundary conditions should be applied to constraint the bottom edge of the new stones, which adds a degree of complexity that is not treated here.

### 4.1.3 Influence of the location of the stone

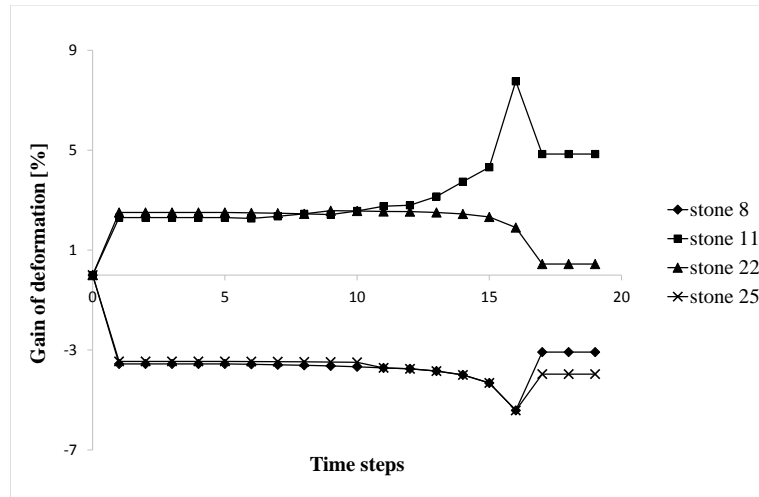
This paragraph deals with the the influence of the position of the stone to be restored relatively to the whole section. For this, 5 different stones are replaced (stones 8, 11, 16, 22 and 25, see Figure 4.2). In the Figure 4.15, it can be observed that the global deformation of the section is always very close to the one caused by the replacement of the middle stone (stone 16). The Figure 4.16 shows the increase of deformation when replacing one of the 4 stones compared to the deformation due to the replacement of the middle stone 16. It leads to the following observations:



**Figure 4.15:** Vertical deformation of the heterogeneous model when restoring 5 different stones

- The closer the stone is to the middle stone, the closer is the deformation (this is the case of stone 22 that touches stone 16). However, the deformation for the very external stones (stone 25 and 8) is not so different (up to 8%) compared to the deformation when stone 16 is replaced. This is the reason why the next study is carried out only for the middle stone, and the results could be adapted for all stones.
- The highest deformation is reached for stones in the columns of the second fifth and the forth fifth of the section. Here, it concerns stones 22 and 11. It seems also logical: in

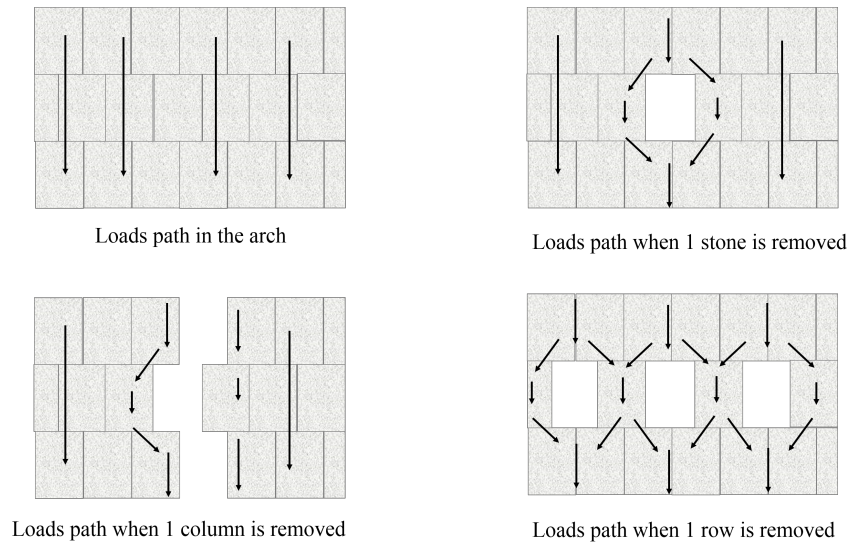




**Figure 4.16:** Increase in vertical deformation compared to the deformation due to the replacement of the middle stone 16

the case when those stones are removed, the load is transferred through two narrower columns (on the left and on the right) than when the middle stone is removed. In this case indeed, the load transfers through two thicker columns, on the left and on the right. In the final configuration, for stones 8 and 25, which are on the external sides, the load transfers through one thick column on the left (stone 25) or on the right (stone 8), so the deformation is small (see Figure 4.17).

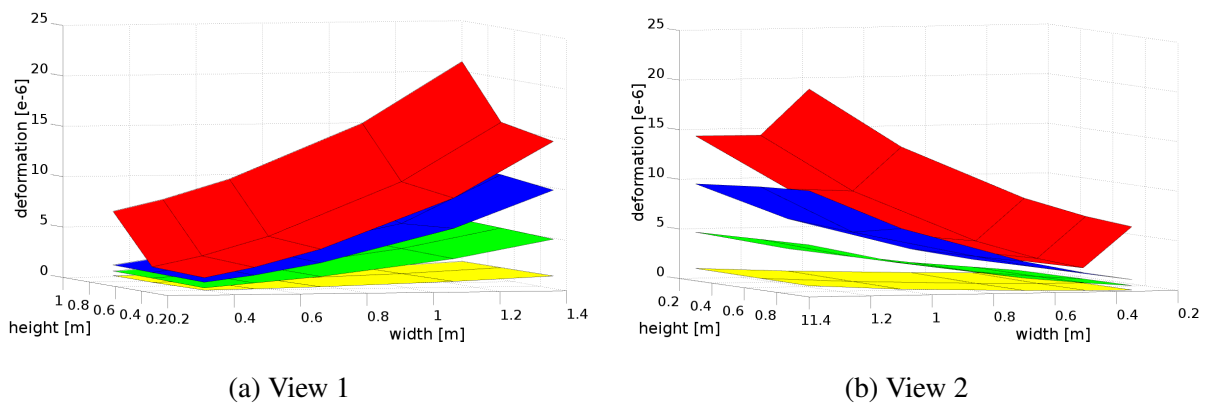
- There is still a slight difference between the deformation due to the removal of stone 8 and 25 in Figure 4.16 due to the fact that the stone 16 is not exactly in the middle but closer to stone 8. In Figure 4.15 on the contrary, the deformation is exactly the same.
- As a conclusion, the stones should be replaced column by column, since the other stones of the column will not be of any help transferring the loads during the replacement. On the contrary, if the different stones of a stage are all in different columns, the deformation would be very high.



**Figure 4.17:** Path of the loads when the stone is removed for different procedures of replacement of the stones

#### 4.1.4 Influence of the size of the stone

In this paragraph, the influence of the size of the replaced stone is examined. For this, 15 cases are studied, for 4 different levels of the replaced stone.



**Figure 4.18:** 3D plot of the deformation of the heterogeneous model for different activation pressures and different sizes of stone (red:  $p = 0$  MPa, blue:  $p = 0.18$  MPa, green:  $p = 0.36$  MPa, yellow:  $p = 0.5$  MPa)

The parameters are:

- The height of the stone:  $H = [0.3 \text{ m}, 0.7 \text{ m}, 1.0 \text{ m}]$
- The width of the stone:  $W = [0.35 \text{ m}, 0.5 \text{ m}, 0.7 \text{ m}, 1.1 \text{ m}, 1.4 \text{ m}]$
- The level of pressure used to activate the replaced stone:

$$p = [0. \text{ MPa}, 0.18 \text{ MPa}, 0.34 \text{ MPa}, 0.5 \text{ MPa}]$$

This means, in term of comparison to the final pressure  $\bar{p} = 0.5 \text{ MPa}$ :

$$p = [0\bar{p}, 0.36\bar{p}, 0.68\bar{p}, \bar{p}]$$

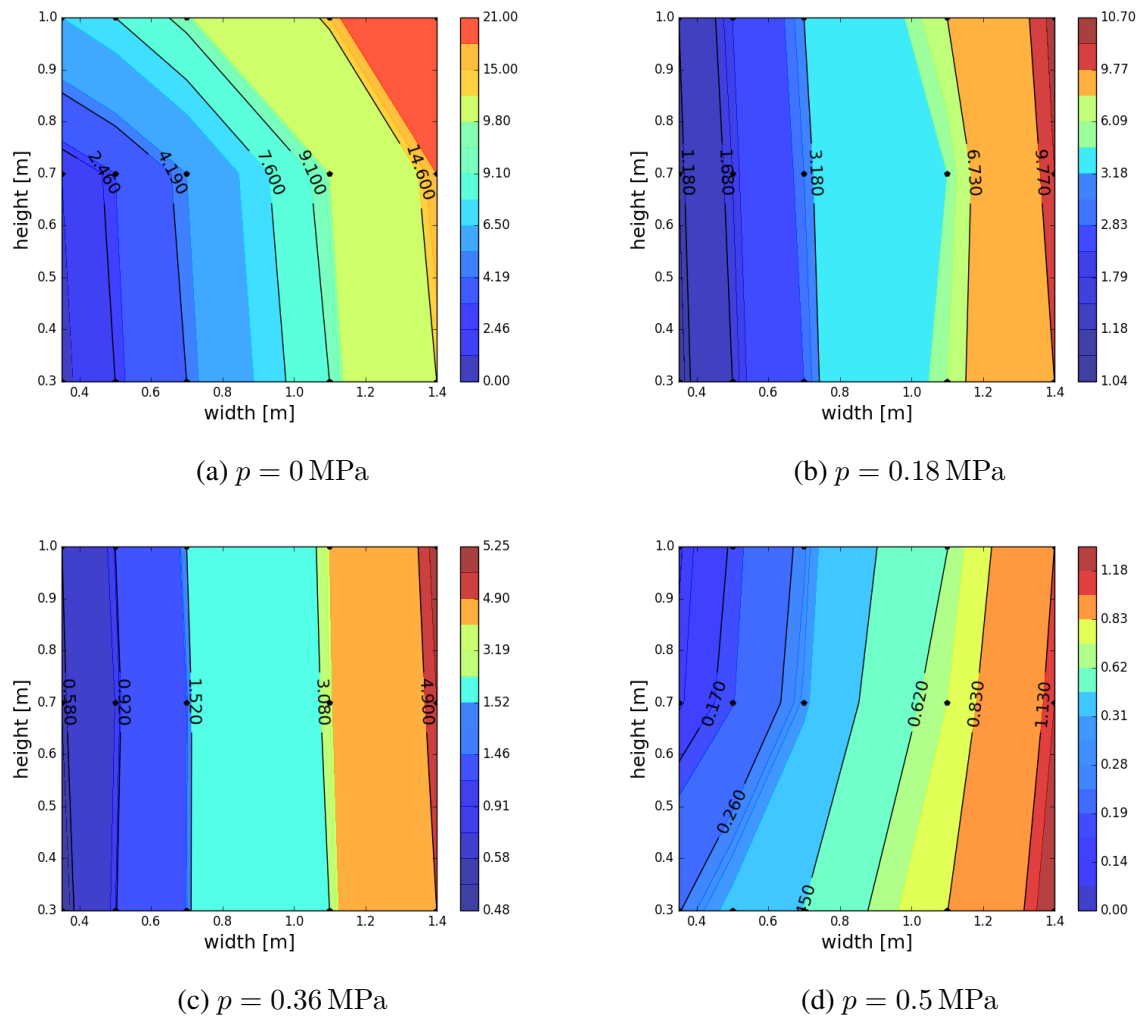
The final value  $H = 1 \text{ m}$  might be disproportionate since it is very rare to use so big stones. However, it should be reminded that the basic stone unit is  $0.5 \times 0.7$  and it was interesting to study the case when the stone was higher than the adjacent ones.

The results are presented in Figures 4.18, 4.19 and 4.20. First, these graphs show that it is very important to follow the activation sequence, which will be discussed later. Then, Figure 4.20a shows that the height of the stone is of little importance: for a given pressure, the global deformation is almost a constant. On the contrary, the width of the stone is a more important parameter. Indeed the deformation for a constant pressure is one order of magnitude bigger for a stone 1.4 m wide compared to 0.35 m.

In the Figure 4.21, we can also observe the state of stress for the two extreme widths of the stone. For the wider stone, the stress concentration is 3 times higher than the initial stress, and 2 times higher than the concentration of stress for the 0.35 m wide stone. This indicates that the wider the stone, the higher the global deformation and local gain of stress. As a consequence, two adjacent stones in on the same row should not be replaced together. This is linked to the consideration that the narrower the columns to be changed, the fewer consequences on the remaining parts of the bridge.

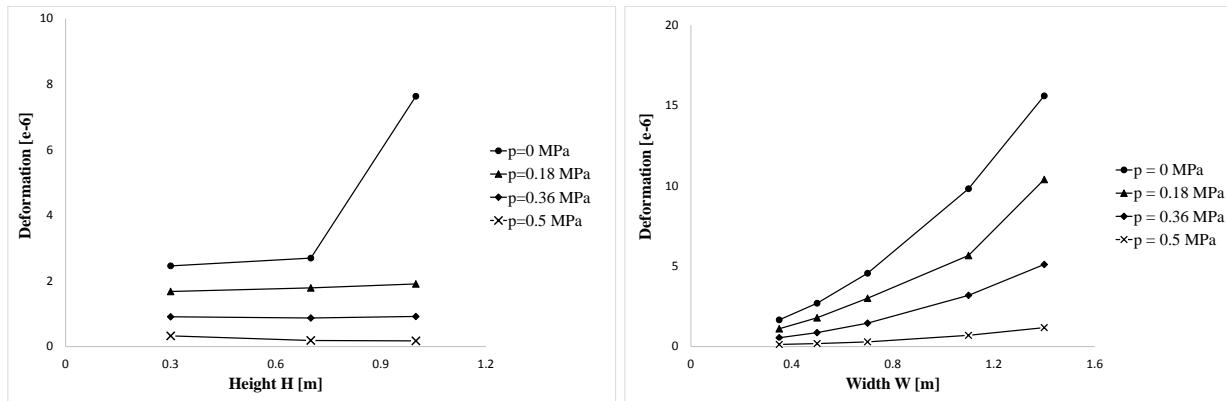
#### 4.1.5 Consequences of the linearity of the model

Finally, this study compares different process of replacement to draw some conclusions from the fact that the analysis and the material are linear. 4 stones are replaced: stone 8, stone 11, stone 22 and stone 25. 4 cases are compared.



**Figure 4.19:** Vertical deformation of the heterogeneous model [ $\times 10^{-6}$ ] for different values of activation pressure and different dimensions of stone (numerical points are marked in black)

1. *4 stages*: the four stones are changed in 4 stages, in the order 22, 25, 8, 11.
2. *4 simultaneously*: the four stones are changed during the same stage.
3. *4 models*: 4 different models are written, one per stone.
4. *Sum of 4 models*: the results of the case *4 models* are summed.



(a) width = 0.5 m, height variation

(b) height = 0.7 m, width variation

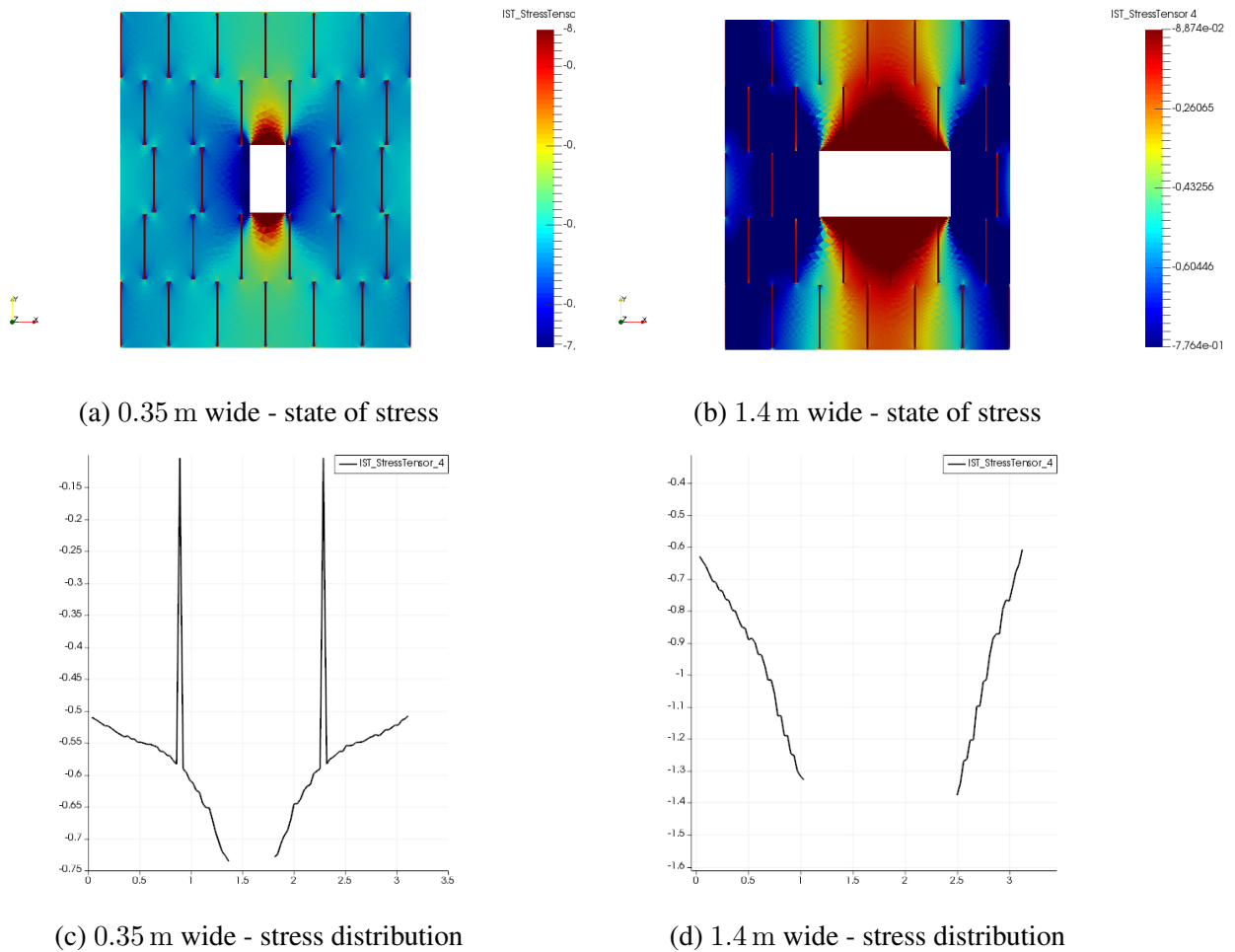
**Figure 4.20:** Deformation of the heterogeneous model for different activation pressures and different dimensions

#### 4.1.5.1 Comparison of 4 stages and 4 models

The difference between those cases is that in the second case, four models where 1 sole stone is replaced are written. There is no initial consequence due to the replacement of previous stones. The time of replacement is the same as in the case *4 stages*, so that they are comparable. The results are presented in Figure 4.22. Obviously, the behavior is the same for stone 22, which is the first one replaced. One shall notice that the gap between maximum deformations (reached when a stone is removed) for the same stone increases with the number of stages, even considering the initial deformation at the beginning of the stage. This fosters the recommendation that the more stones of a column can be replaced in one stage, the better for the overall deformation.

#### 4.1.5.2 Comparison of 4 stages, 4 simultaneously and sum of 4 models

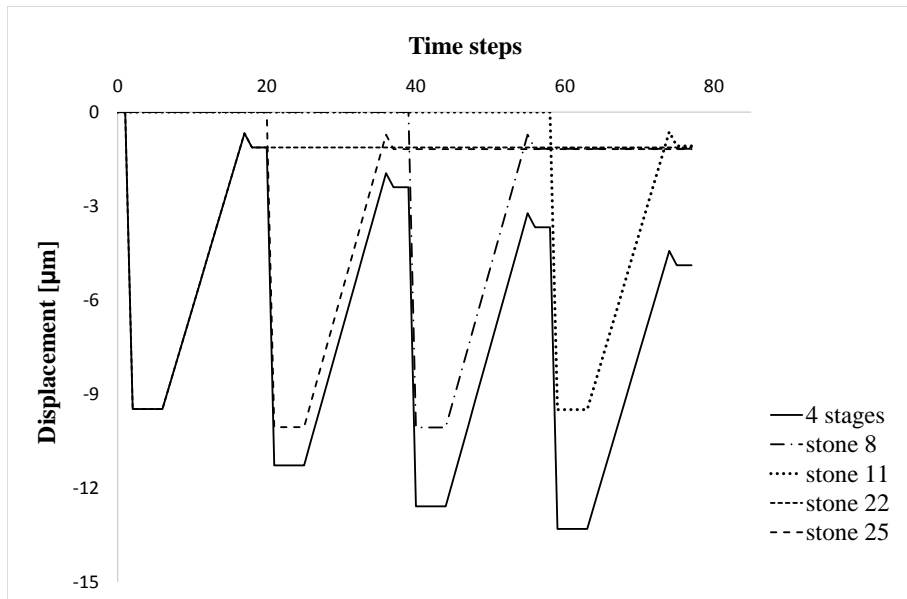
The graphs of those three cases are presented in Figure 4.23. Here, a sum of the deformation due to the replacement of each stone was applied to the cases *4 models* and *4 stages* so that it is possible to compare it with the case *4 simultaneously*. The case *4 simultaneously* is the worst one, and is an upper envelope to the *4 stages*. The maximal deformation represents 116% of the *4 stages* case, and the final deformation 107% of it. The case *4 models* minimizing the de-



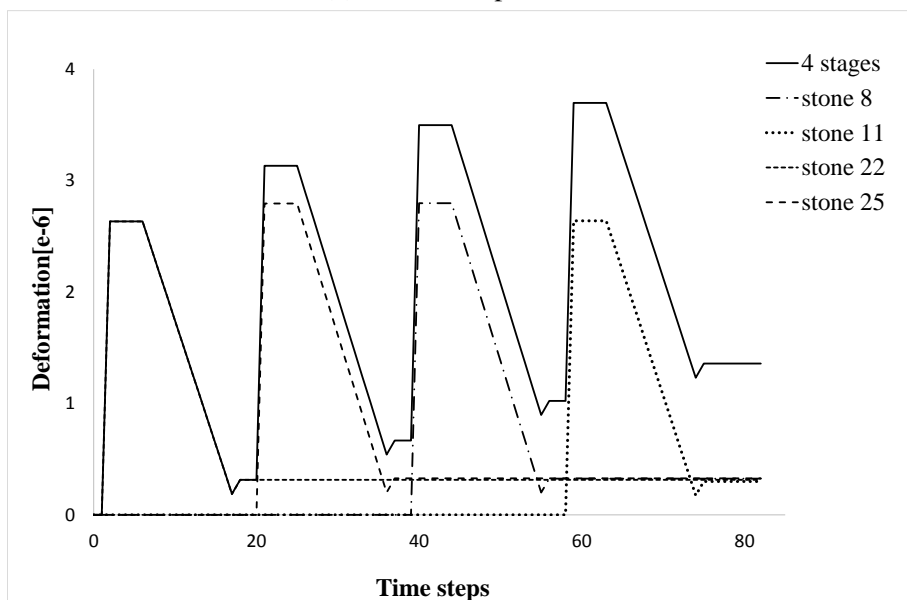
**Figure 4.21:** State of stress [MPa] for the two extreme widths of a stone examined (0.7 m high)

formation, and is a lower envelope to the case *4 stages*. The maximum deformation represents 99% of the *4 stages* case, and the final deformation 93% of it (see Table 4.1).

The case of *4 stages* should be the closest to what actually happens when replacing a stone. However, it is interesting to notice that with a linear analysis, the results are very close to the one of an analysis where the stones are all replaced in one stage, or to the one when only one stone is studied in the model. This enables a quick overview of the consequences of a replacement, with very easy modeling. Indeed, as it was discussed earlier, the more stages, the more complex the model. As the modeling file is written for now, it is even impossible to apply it to the whole



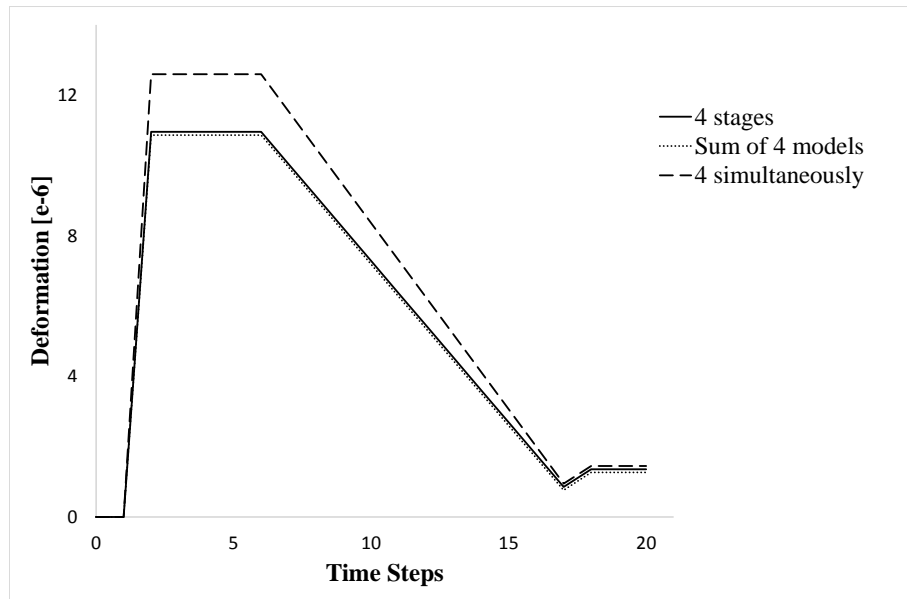
(a) Vertical displacement



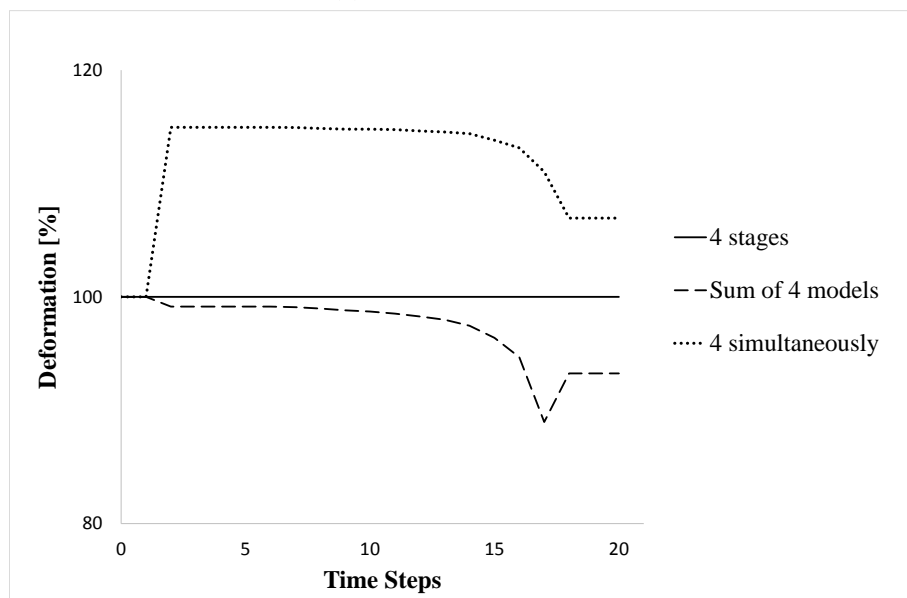
(b) Deformation

**Figure 4.22:** Comparison of the behavior of the heterogeneous model when using 4 stages in one model or 4 models of 1 stage

arch. Using these consideration would enable engineers to have a first idea of the maximum and final deformation of the structure.



(a) Vertical deformation



(b) Comparison in percentage

**Figure 4.23:** Comparison of the behavior of the heterogeneous model when using 4 stages in a model, 4 models of 1 stage, and the sum of the results of the previous 4 models

#### 4.1.6 Importance of the activation process

Finally, the importance of a good activation process is discussed. On site, this concerns the attention paid to the wooden wedges installation, and most of all to wait until the mortar has



Table 4.1: Comparison of the deformation in the heterogeneous model when using 4 stages in a model, 4 models of 1 stage, and the sum of the results of the previous 4 models

deformation	sum of 4 models	4 stages	4 simultaneously
when removing the stone [1e-6]	10.86	10.96	12.60
when removing the stone [%]	99	100	115
final state [1e-6]	1.27	1.36	1.45
final state [%]	93	100	107

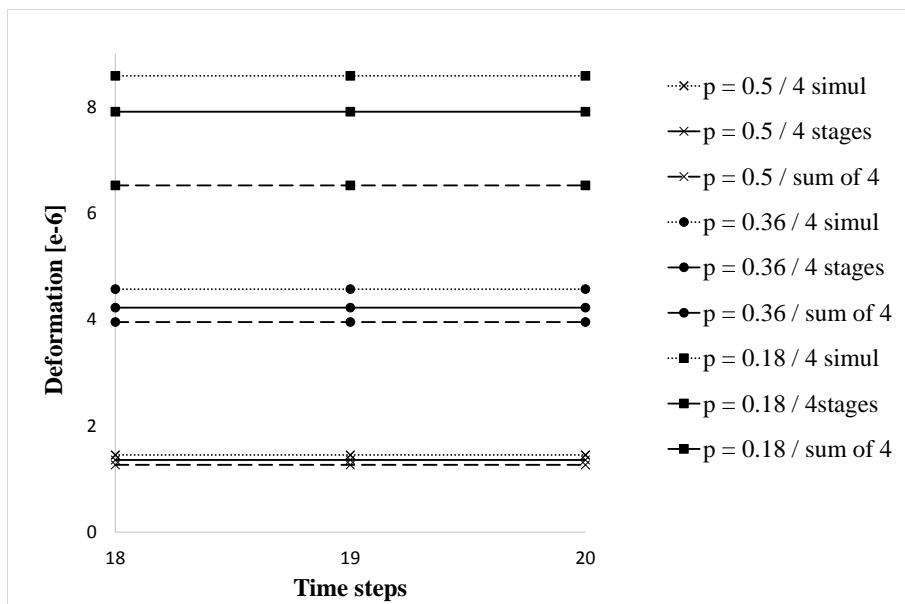


Figure 4.24: Vertical deformation of the heterogeneous model for different activation pressures when using 4 stages in a model, 4 models of 1 stage, and the sum of the results of the previous 4 models

hardened before removing them. Though it is necessary, the hardening of mortar is one of the most influencing parameters on the global time of work.

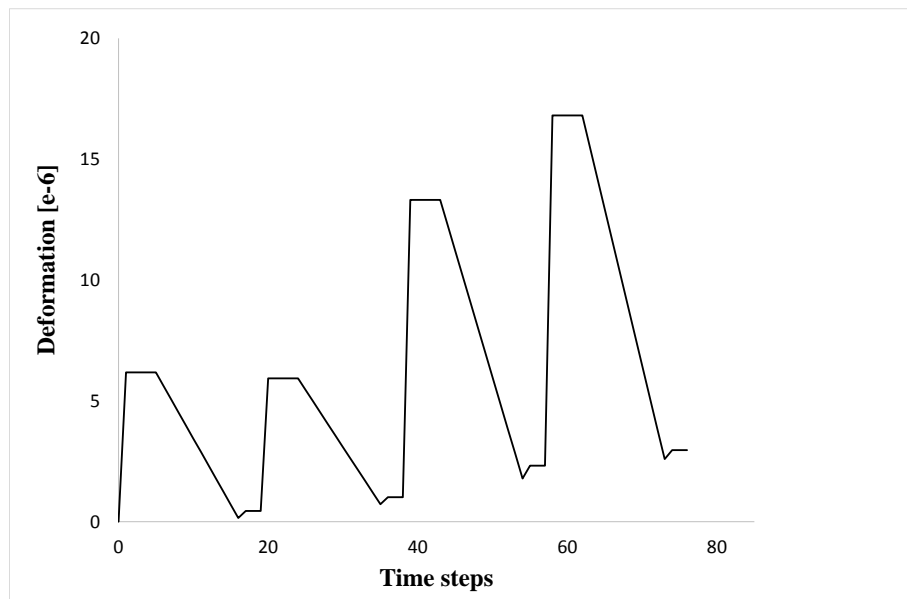
In Figure 4.20, if the activation pressure is close to 0.5 MPa – which means that the new stone experiences the same level of stress as the adjacent stones – the deformation is smaller. Respect of this activation step of the process is therefore very important for the minimization of the global deformation.

In Figure 4.24, it is clear that the smaller the activation pressure, the bigger the gap between

the different cases examined. As explained earlier, it can be a great gain in design time to consider the model with only one stone being removed. However, this can be verified only if the activation process is respected on site. Otherwise the damage for the arch might be way more important than the one predicted.

## 4.2 Application to the reduced area of arch

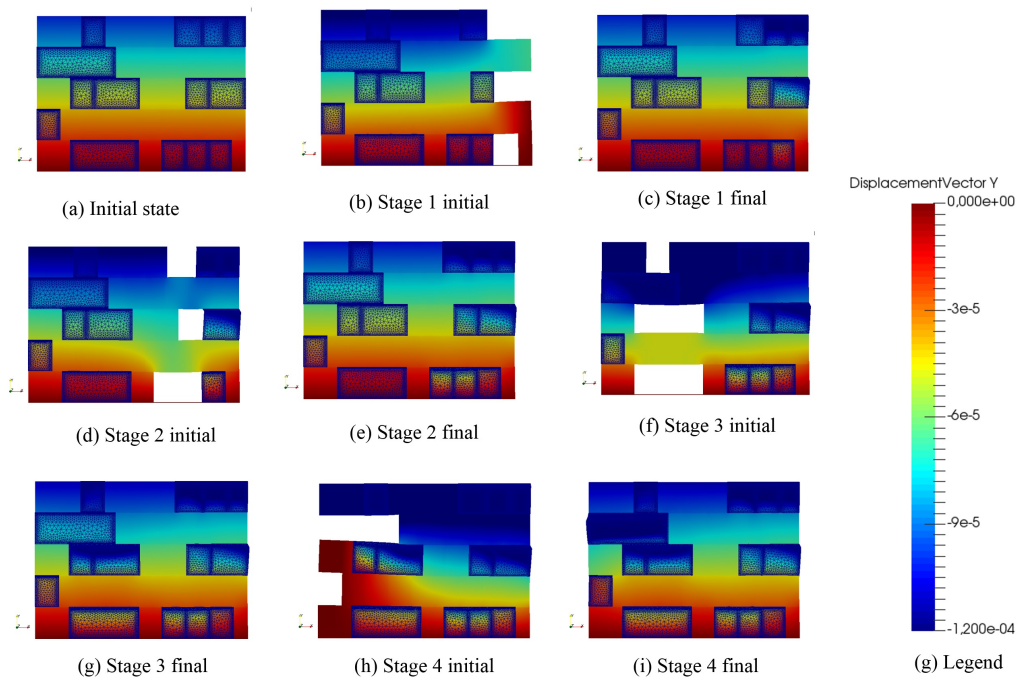
Finally, the current modeling strategy is applied to the investigated area of arch. The geometry of the model is closed to the geometry presented in the previous chapter.



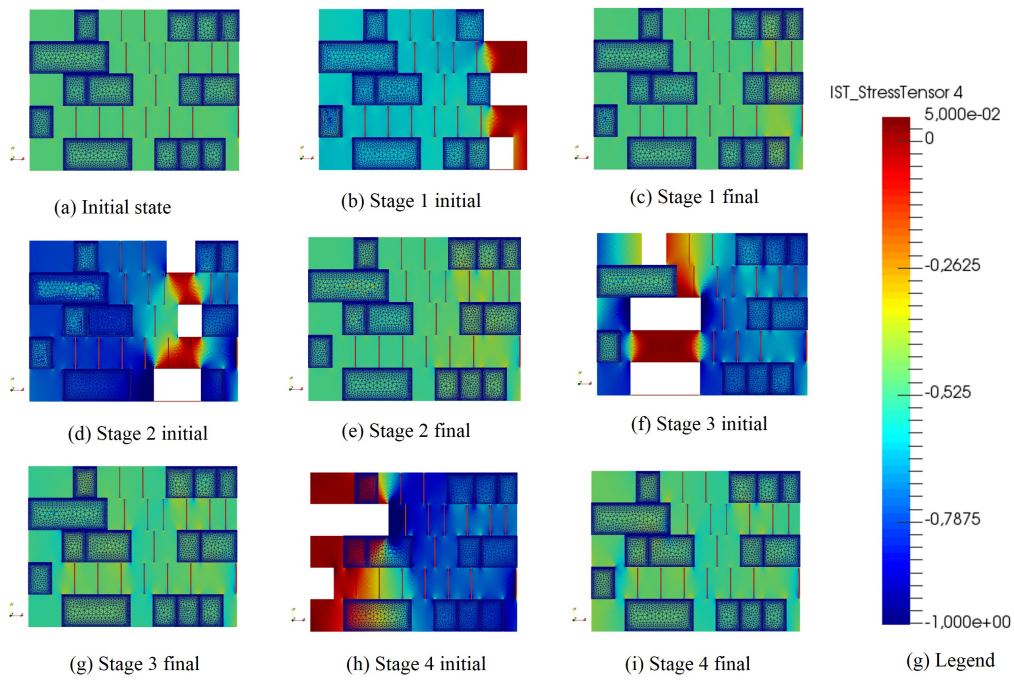
**Figure 4.25:** Vertical deformation of the examined reduced area in time

The same stones are replaced as in the previous model, here numbered: 38, 37, 22, 6, 36, 21, 4, 5, 32, 17, 18, 2, 23, 8. The section is divided into 4 columns, and the complete restoration is done in 4 stages. Because of the geometry of the stones, it was hard to define the combinations for all stages. A further study would consist in optimizing the procedure.

The Figures 4.26 and 4.27 presents the states of displacement and stress. In the graph 4.25 is the deformation of the model.



**Figure 4.26:** Vertical deformation [m] of the examined reduced area



**Figure 4.27:**  $\sigma_{yy}$  stress [MPa] in the examined reduced area

### 4.3 Limits of the model

This heterogeneous model can capture the procedure of reactivation of the new stones. Therefore, it can be used to study local increase of stress. It appears that under the assumption of linear elastic analysis, and for the case when the activation process is respected (fulfilled pressure on the newly inserted stone), simplification in the methodology can be used. Instead of creating one model of  $N$  stages,  $N$  models of one stage each describe quite well the final results. Its strongest drawback currently is the fact that it is very complex to prepare and that the possibilities of geometry and of number of stages is very limited. The investment of time to prepare the model might not be worthy; therefore it would be interesting to develop an automatic tool to print the geometry and the stages. Another limit of the current model is the linearity of the material. Further studies should be carried out to treat the case of non-linear material.

## Conclusion

The current work led to the development of two methodologies to model the intrados of the Charles Bridge in order to optimize the replacement procedure of the most weathered stones.

In order to have a low impact on the existing structure, the constraints are the minimization of the axial shortening as well as the prevention of local increase of stress around the replaced stone, or development of tensile stress. The specific points that the models can capture are the intervention in stages – and consequently changes in the static scheme – as well as the process of reactivation to transfer the loads from the structure to the new block.

Only a representative area of the most damaged masonry arch is examined: 5 rows of 7 to 9 blocks of sandstone (3.5 m × 4.5 m). It is modeled as an unfolded 2D element loaded in the vertical plane, as a plane stress problem. The reduced area is simply supported on its bottom edge, and free of constraint on lateral edges; no additional friction due to the connection with the bridge is added. The material constituting the masonry behaves linearly. The geometry is implemented with semi-automatic scripts using Matlab and Python. The linear elastic finite elements calculation is performed with the software OOFEM.

One model is homogeneous and isotropic. It is really simplified due to this homogeneity. Because of the fact that each weathered stone must be implemented by hand, the geometry of the blocks is rough. It is not satisfactory to capture the reactivation phenomenon and to describe the behavior around the stone: the local increase of stress and the development of tensile stress is not accurate. The solution proposed to model the local scale uses eigenstrain activation of the stone and needs to be applied manually for each block dimension and stiffness, which is not suitable for more than four or five damaged stones.

Nonetheless, the homogeneous model is efficient to capture the global behavior of the arch. Indeed, it gives consistent results concerning the axial shortening, even without the reactivation of the units. Since the computational time is very low, it can be used to get a rough idea of the response of the arch when replacing some stones.

Another model takes into account the mesostructure of masonry by modeling the layers

of 0.02 m of mortar. It can describe the replacement procedure step by step, including the reactivation of a stone after the removal of the damaged one. Nonetheless, it is complex to create and only a limited number of stages can be currently implemented because the input file is semi-automatic. Since the analysis is only linear elastic, optimization must be performed before using it more widely.

The heterogeneous model can be used to study the local response of the arch during the replacement process, to minimize the local increase of stress around the stone and to check that no tensile stress develops. Though the modeling can become complex, it was shown that under the assumption of linear elastic analysis, very similar results are obtained when replacing the stones in one stage, or creating as many models as the number of stones and summing the results of the four models. This remark only applies when the reactivation is complete and the final stress in the new stone is the same as in the structure.

The methodology that was developed with these models is satisfactory to model the phases of the intervention stage by stage, with corresponding changes in properties of the stone, in boundary conditions and in static scheme. The reactivation procedure is also captured in the second model by means of the application of a uniform distributed load on the newly inserted stone.

Some recommendations can already be drawn out of the present work to optimize the procedure of restoration.

- The stones should be replaced column by column since the loads transfer through lateral elements of masonry when a stone is removed.
- On the contrary, too many stones in the same row shall not be replaced during the same stage.
- The procedure of reactivation must be followed strictly: if the reactivation pressure is not high enough, the impact on the structure is not minimized.
- A combination of both models can be used. With the homogeneous model, a replacement procedure that minimizes the global deformation can be established. The heterogeneous

model is then used to validate the procedure from the point of view of local increase of stress around the removed stones.

- Under the condition that the activation procedure is respected (full activation pressure applied), the heterogeneous model gives similar results when creating one model with four different stages or four different models with one stage. This solution, that is easier and low time demanding, can be applied to optimize the replacement procedure.

## Perspectives

Further studies could be carried out with these models to understand the *influence of certain parameters* on the global deformation:

- the maximum width of a column of stones that can be removed during one stage, compared to the width of the restored area,
- the maximum area of stone that can be replaced during one stage, compared to the area that requires restoration,
- the minimum number of stages that are needed to replace all the stones.

The results coming from these studies might enable to *establish criteria* on the maximal deformation that the arch can suffer to guide engineers in the preparation of site intervention.

For a wider application of the present models, the *computational codes must be optimized*. Both the complexity of the geometry and high number of stages cannot be treated for now. Other studies should be carried out to treat the case of *non linear material*.

The specificity of these numerical solutions is that they can model a site procedure which has a temporary though strong impact on the structures. In the case of historical heritage, where the material in place shall be conserved as remains of the past, such modeling is very interesting to prepare an optimized site work. Because the arch was modeled unfolded with plane stress hypothesis, the present results can be applied to *any wall loaded in its plane*.

Another specific aspect of this methodology is the modeling of stages to reflect the different *phases of construction on site*. A set of time functions rules the presence or absence of

finite elements and their properties. Such modeling strategy, in stages, can be applied to other engineering fields: the construction in general, but also mechanics.



# References

- [1] Charles bridge museum in prague. <http://www.prague-bridge.com/>, 2017.
- [2] Climate data in europe. <https://climate-data.org/location/6286/>, 2017.
- [3] Oofem website. <http://www.oofem.org/doku.php?id=en:oofem>, 2017.
- [4] M André, Bruno Phalip, Olivier Voldoire, Erwan Roussel, Franck Vautier, and David Morel. Quantitative assessment of post-restoration accelerated stone decay due to compatibility problems (st. sebastian’s abbey church, manglieu, french massif central). 2012.
- [5] W. Bangerth, R. Hartmann, and G. Kanschat. Deal.ii—a general-purpose object-oriented finite element library. *ACM Trans. Math. Softw.*, 33(4), August 2007.
- [6] Wolfgang Bangerth, Ralf Hartmann, and Guido Kanschat. deal. ii—a general-purpose object-oriented finite element library. *ACM Transactions on Mathematical Software (TOMS)*, 33(4):24, 2007.
- [7] Boleslav Běžina and Michal Kindl. Oprava karlova mostu, etapa 0003 - doplňující stavebně-technický průzkum oblouku č.14. *PUDIS akciová společnost*, 2007.
- [8] Tim De Kock, Wesley De Boever, Jan Dewanckele, MA Boone, Patric Jacobs, and Veerle Cnudde. Characterization, performance and replacement stone compatibility of building stone in the 12th century tower of dudzele (belgium). *Engineering Geology*, 184:43–51, 2015.
- [9] Richard Fawcett. The conservation of architectural ancient monuments in scotland guidance on principles. *Historical Scotland*, 2001.

- [10] Tea-Sung Jun and Alexander M Korsunsky. Evaluation of residual stresses and strains using the eigenstrain reconstruction method. *International Journal of Solids and Structures*, 47(13):1678–1686, 2010.
- [11] Petr Kabele, Milan Jirasek, and Paulo B Lourenço. *SAHC Master lectures - SA2 : structural analysis techniques*. SAHC Consortium, 2017.
- [12] Tomáš Krejčí and Jiří Šejnoha. Evolution of temperature and moisture fields in charles bridge in prague: Computational prediction and measurements. *International Journal of Architectural Heritage*, 9(8):973–985, 2015.
- [13] PB Laurenco, Jan G Rots, and Johan Blaauwendraad. Two approaches for the analysis of masonry structures: micro and macro-modeling. 1995.
- [14] Paulo B Lourenco, Gabriele Milani, Antonio Tralli, and Alberto Zucchini. Analysis of masonry structures: review of and recent trends in homogenization techniques this article is one of a selection of papers published in this special issue on masonry. *Canadian Journal of Civil Engineering*, 34(11):1443–1457, 2007.
- [15] Nirvan Chandra Makoond. Advanced computational modelling of taq-kisra, iraq. Master’s thesis, Czech Technical University in Prague, SAHC Advanced Master’s Consortium, 2015.
- [16] MATLAB Manual. the mathworks. *Inc., Natick, MA*, 1995.
- [17] Gihad Mohamad, Paulo B Lourenço, and Humberto R Roman. Poisson behaviour of bedding mortar under multiaxial stress state. 2006.
- [18] SP Narayanan and M Sirajuddin. Properties of brick masonry for fe modeling. *American Journal of Engineering Research (AJER)*, pages 2320–0847, 2013.
- [19] Borek Patzák. Oofem element library manual. 2016.
- [20] Bořek Patzák and Z Bittnar. Oofem—an object oriented framework for finite element analysis. *Acta Polytechnica*, 44(5-6), 2004.

- [21] Bořek Patzák and Zdeněk Bittnar. Design of object oriented finite element code. *Advances in Engineering Software*, 32(10):759–767, 2001.
- [22] Richard Příkryl, Zuzana Weishauptová, Miroslava Novotná, Jiřina Příkrylová, and Aneta Št'astná. Physical and mechanical properties of the repaired sandstone ashlar in the facing masonry of the Charles Bridge in Prague (Czech Republic) and an analytical study for the causes of its rapid decay. *Environmental Earth Sciences*, 63(7-8):1623–1639, 2011.
- [23] WJ Quist. Replacement of natural stone in conservation of historic buildings. *Heron*, 54(4):251–278, 2009.
- [24] Daniel Rypl. T3d - triangulation of 3d domains user guide. *Czech Technical University in Prague - Faculty of Civil Engineering, Department of Mechanics*, 2012.
- [25] Massimo Toesca. Thermo-mechanical analysis of the Charles Bridge in Prague. SAHC dissertation, CVUT – Prague, 2014.
- [26] Jan Zeman, Jan Novák, Michal Šejnoha, and Jiří Šejnoha. Pragmatic multi-scale and multi-physics analysis of Charles Bridge in Prague. *Engineering Structures*, 30(11):3365–3376, 2008.